A behavioural–environmental model to study the impact of climate change denial on environmental degradation

A behavioural–environmental model to study the impact of climate change denial on environmental degradation

Kathinka Frieswijk[a,b], Lorenzo Zino[c], A. Stephen Morse[d], Ming Cao[a]

[a] *Engineering and Technology Institute Groningen, University of Groningen, Nijenborgh 4, Groningen, 9747 AG, The Netherlands*
[b] *Public Health Service of Groningen (GGD Groningen), Hanzeplein 120, Groningen, 9713 GW, The Netherlands*
[c] *Department of Electronics and Telecommunications, Politecnico di Torino, Corso Duca degli Abruzzi 24, Torino, 10129, Italy*
[d] *Department of Electrical Engineering, Yale University, 17 Hillhouse Ave, New Haven CT, 06511, US*

Abstract

Climate change is the biggest global threat facing humanity in the coming decades. The scientific community agrees that human activity has been responsible for virtually all global heating over the past two centuries, emphasising the urgent need for the collective adoption of environmentally responsible behaviour. In this paper, we propose a novel behavioural–environmental mathematical model that explores the complex and nonlinear co-evolution of human environmental behaviour and anthropogenic environmental degradation. Our model considers a population of individuals, which includes climate change deniers, interacting on a polarised population structure. In addition to addressing climate change denial, our framework captures other key aspects of the climate crisis by modelling human behaviour through a social learning mechanism inspired by game theory that accounts for social influence, environmental sensitivity, government policies, and the costs associated with environmental-friendly actions. By employing a mean-field approach in the limit of large populations,

*Corresponding author L. Zino (email: `lorenzo.zino@polito.it`)
Email addresses: `kathinka.frieswijk@ggd.groningen.nl` (Kathinka Frieswijk), `lorenzo.zino@polito.it` (Lorenzo Zino), `as.morse@yale.edu` (A. Stephen Morse), `m.cao@rug.nl` (Ming Cao)

we derive an analytically tractable set of equations that is easy to simulate. By analysing this set of equations, we shed light into the emergent behaviour of the system. Under reasonable assumptions, we demonstrate global convergence to a periodic solution, with oscillations influenced by climate change deniers and polarisation in a non-trivial manner, as discussed via a campaign of numerical simulations.
Keywords: climate change, human behaviour, mean-field, modelling, nonlinear ODEs, oscillatory behaviour

1. Introduction

Climate change is the biggest global threat of the century, endangering human beings and millions of other species. Over recent decades, Earth's climate has experienced substantial changes, primarily due to human activities releasing greenhouse gases into the atmosphere [1]. These changes have far-reaching consequences, including a massive increase in the frequency and severity of droughts, floods, wildfires, and storms [2, 3], resulting in widespread food insecurity, significant disruptions in agricultural production, and substantial harm to livelihoods [4].

To avoid the most damaging consequences of the climate crisis, there is agreement in the scientific community that a collective adoption of environmentally responsible behaviour is necessary [5]. Under the Paris Agreement of December 2015, the vast majority of the world's nations committed to limiting the rise in the average global temperature to well below 2°C above pre-industrial levels while pursuing efforts to cap the increase at 1.5°C [6]. However, a special report issued in 2018 by the Intergovernmental Panel on Climate Change emphasised the need to limit the increase in temperature to 1.5°C, as crossing this threshold unleashes significantly more severe environmental impacts [7]. Currently, we are surpassing this threshold, with the global average temperature for the period April 2023 – March 2024 reaching 1.58°C above the pre-industrial average [8]. The climate crisis has already inflicted substantial and often irreversible damage

on numerous ecosystems, leading to biodiversity loss [2, 9].

Climate policies typically target sectors with high emissions, such as air travel, industry, housing, agriculture, and the automotive industry. While this focus is politically justifiable, it overlooks a crucial aspect of emission dynamics: the choices of individual households. Household consumption behaviour and lifestyles are related to 72% of emissions [10, 11]. For example, consider the popularity of large, heavy, and environmentally unfriendly 'Sports Utility Vehicles' (SUVs), which accounted for around 46% of global car sales in 2022 [12]. While one could attribute the high SUV emissions to the companies manufacturing these vehicles, it is essential to recognise that individual consumers actively choose to purchase such polluting cars. In 2022, the collective global fleet of 330 million SUVs emitted nearly 1 gigatons of CO_2 [12]. Individuals can reduce transport emissions by making pro-environmental choices like avoiding air travel, prioritising public transportation over individual car usage, and opting for electric vehicles instead of petrol or diesel cars. Besides transport emissions, another example relates to the food individuals consume. Roughly one-third of global anthropogenic greenhouse gas (GHG) emissions stem from activities related to the food industry [13]. The livestock industry accounts for the majority of these emissions [14]. Beef production, in particular, has a substantial environmental footprint, accounting for a quarter of emissions associated with food production alone [14]. Achieving adequate mitigation of GHG emissions requires a global shift towards healthier, plant-based diets [15], which would reduce global food-system GHG emissions by 49% [16].

With the rapid rise in temperature and extreme weather conditions all around the globe in recent years, it is hard to deny that climate change is a serious and real threat to all life on our planet. Nevertheless, despite the overwhelming amount of scientific evidence [2, 3, 4, 7, 17, 18], there still exists a small minority of individuals who maintain beliefs denying the reality of human-caused climate change [19]. In a survey conducted by the European Commission in May–June 2023, it was found that 76% of Europeans perceive climate change as a very serious problem, 17% view it as a fairly serious problem, and 7% do

not consider it a serious problem [20]. In the United States, climate change denial is particularly present, fuelled by an anti-environmental counter-movement heavily funded by the fossil fuel industry, conservative activists, and conservative foundations [21, 22, 23, 24, 25]. Initially, this counter-movement involved spreading misinformation and promoting supposed "uncertainty" regarding the existence and severity of climate change [26]. Over time, the denial campaign evolved to include direct attacks on climate science and the integrity of climate scientists [27]. Consequently, there is widespread scepticism and outright denial among the public and policymakers—impeding the adoption and implementation of effective measures to address climate change [22].

When interacting with others, individuals often exhibit *homophily*, i.e., the tendency to interact with people sharing similar beliefs [28, 29, 30]. On the topic of climate change, most individuals interact only with like-minded others on social media platforms [31]. This selective exposure to information fosters echo chambers and polarises public opinion [32, 33]. Over the years, public opinion on climate change has become increasingly polarised, with political liberals generally showing greater acknowledgement of human-caused climate change compared to their conservative counterparts [19, 34, 35, 36].

To accurately study the evolution of environmental behaviour within a population, it is crucial to develop models that capture the complex and nonlinear individual-level mechanisms driving behavioural decisions. Models inspired by game theory offer a promising framework for this purpose [37, 38], as evidenced by their successful adoption in various real-world applications, spanning from social dynamics [39, 40] to the behavioural response to epidemic spreading [41, 42]. For instance, to study the evolution of cooperative behaviour, the researchers in [43] employ a framework incorporating the Prisoner's Dilemma and Snowdrift games, introducing punishment as an additional strategy to deter selfish defectors from free-riding. However, their model assumes constant strategy payoffs independent of a changing external environment, which limits its applicability in modelling climate change and human behavioural responses. In a recent study [44], a coupled evolutionary framework is proposed to study the

evolution of forest degradation and human mitigation decisions, whose payoffs depend on temperature forecasts. Simulations reveal various evolutionary outcomes, ranging from long-term system oscillations in both mitigative behaviour and vegetation coverage to complete forest depletion. This study does not, however, account for polarisation and climate change denial. Also of interest is the paradigm of feedback-evolving games, where individual behaviour and the environment do mutually influence each other [45, 46, 47, 48, 49]. While feedback-evolving games successfully explain dynamic phenomena in biological systems, such as resource harvesting and plant nutrient acquisition [50], these approaches typically rely on the simplifying assumption that individual decision-making is governed by a convex combination of two payoff matrices, with the environmental state as the parameter weighting the two matrices. Consequently, these games cannot capture heterogeneity, as well as more complex and nonlinear features present in human decision-making, limiting their practical applicability.

To bridge this gap, we propose a novel behavioural–environmental model for the co-evolution of anthropogenic environmental impact and human behaviour. In the proposed model, individuals revise their behaviour according to a social learning mechanism in which they tend to imitate their peers with a larger reward [38]. In particular, individuals' rewards are designed to capture real-world incentives to adopt or not adopt sustainable behaviours and are thus affected by several factors, including social influence (which substantially affects pro-environmental behaviour [51, 52, 53, 54]), sensitivity to the environmental degradation, implementation of governmental policy interventions, and higher costs associated with environmentally friendly behaviour. To model the phenomenon of climate change denial, we expand the single-population behavioural–environmental model that appeared in our earlier preliminary work [55] to a more realistic multi-population scenario accounting for the polarised public opinion on climate change. Here, we introduce a parameter representing individuals' level of homophily. The higher the level of homophily, the higher the probability of interaction and imitation of individuals with a similar belief, capturing the well-known phenomenon of conforming

to the behavioural norm within one's social environment [56]. Formally, our mathematical model consists of a high-dimensional non-homogeneous Markov process [57], coupled with a non-linear ordinary differential equation (ODE) that describes the evolution of the environmental degradation. In summary, our approach advances the state-of-the-art environmental–behavioural models described above [44, 45, 46, 47, 48, 49, 50] by incorporating two important features of human behaviour that were previously neglected (namely heterogeneity and homophily), while also accounting for the presence of peer pressure, which was already considered in [55]. In this way, this model bridges the gaps between behavioural science, environmental studies, and mathematical modelling described above.

In addition to formulating the novel mathematical model and deriving its dynamics, this paper makes three main contributions. The first significant contribution is the adoption of a mean-field approach to analyse the emergent behaviour of the proposed model in the limit of large populations. Specifically, following the approach outlined in [58] and under the assumption of all-to-all interactions within the population, we derive a deterministic approximation of the system's behaviour. This approximation accurately matches the emergent behaviour of large-scale stochastic systems, as demonstrated by theoretical guarantees [59, 60] and supported by numerical simulations. The deterministic approximation consists of a set of non-linear ODEs. Such a system of ODEs lends itself well to analytical treatment and facilitates fast simulations, thus enabling theoretical and numerical studies. Second, we use the deterministic approximation to conduct a theoretical analysis of the system's asymptotic behaviour. Analytically, we consider the case of complete homophily—where individuals exclusively imitate like-minded peers. For this scenario, we compute and characterise the unique interior equilibrium and, utilising a system-theoretic argument based on the Poincaré-Bendixson theorem [61], we establish the emergence of periodic oscillations. In this context, deriving a deterministic mean-field approximation of the Markov chain is essential for establishing novel analytical insights into the system's asymptotic behaviour, as well as for supporting and

complementing results obtained through numerical simulations. Third, we use the system of ODEs to investigate the impact of homophily on the system's behaviour. The low-dimensionality and deterministic nature of our mean-field equations allow extensive exploration of how the presence and quantity of climate change deniers, along with partial homophily within the population, affect the emergent system behaviour and environmental degradation. Interestingly, our numerical simulations depict a scenario that is non-trivial and, to some extent, counter-intuitive. In fact, under the assumptions of our model, it seems that if climate change deniers are marginalised, then their presence could even be beneficial since their actions may cause the rest of the population to react faster to the climate change threat, resulting in smaller oscillations in the environmental degradation. However, such a conclusion should be taken with extreme caution: even a small minority of deniers, when not marginalised, may seriously jeopardise the effort of the rest of the population in protecting the environment.

The rest of this paper has the following organisation. In Section 2, we present some mathematical preliminaries used throughout the paper. Section 3 introduces our multi-population modelling framework. In Section 4, we take a mean-field approach in the limit of large populations and derive the mean-field system dynamics. Section 5 presents our main theoretical and numerical results. Finally, Section 6 discusses future research avenues.

2. Notation and preliminaries

Before presenting the model, we summarise the notational conventions used throughout the paper and present the mathematical preliminaries. Let $\mathbb{R}$, $\mathbb{R}_{\geq 0}$, and $\mathbb{R}_{>0}$ denote the sets of real, non-negative real, and strictly positive real numbers, respectively. The sets $\mathbb{Z}_{\geq 0}$ and $\mathbb{Z}_{>0}$ denote the set of non-negative and strictly positive integer numbers, respectively. Given a set $\mathcal{S}$, $|\mathcal{S}|$ denotes its cardinality, i.e. the number of elements in the set. Given a function $x(t)$ with $t \in \mathbb{R}_{\geq 0}$, we define $x(t^+) = \lim_{s \searrow t} x(s)$, and $x(t^-) = \lim_{s \nearrow t} x(s)$. Given

an event E, we denote by $\mathbb{P}[E]$ the probability that E occurs. Given a random variable X, we denote its expected value by $\mathbb{E}[X]$. Finally, we summarise the following definitions and properties related to stochastic processes, referring interested readers to [57] for more details.

Definition 2.1 (Poisson clock)**.** *A Poisson clock with rate $\rho(t) : \mathbb{R}_{\geq 0} \to \mathbb{R}_{\geq 0}$ is a continuous-time stochastic process, represented by its counting process $N(t) \in \mathbb{Z}_{\geq 0}$. Specifically, $N(t)$ is a non-decreasing function that satisfies the following relation:*

$$\mathbb{P}[N(t + \Delta t) - N(t) = 1] = \int_t^{t+\Delta t} \rho(t)\,\mathrm{d}t + o(\Delta t)\,, \tag{1}$$

for any $\Delta t \in \mathbb{R}_{>0}$, where the Landau little-o notation $o(\Delta t)$ is associated with the limit $\Delta t \searrow 0$. In other words, $\lim_{\Delta t \searrow 0} \frac{1}{\Delta t}\mathbb{P}[N(t + \Delta t) - N(t) = 1] = \rho(t)$. If $N(t)$ has an increment at time $t \in \mathbb{R}_{\geq 0}$, we say that the clock ticks at time t.

Proposition 2.1. *The following properties hold true:*

1. *Let E be an event triggered by the first tick of any clock of a set of independent Poisson clocks with rates $\rho_1(t), \ldots, \rho_\ell(t)$. Then, E can be described as an event triggered by a Poisson clock with a rate of $\rho_E(t) := \sum_{h=1}^{\ell} \rho_h(t)$;*

2. *Let E be an event that occurs with probability $p \in [0, 1]$ if an independent Poisson clock with a rate of $\rho(t)$ ticks. Then, E can be described as an event triggered by a Poisson clock with a rate of $\gamma_E(t) := p\rho(t)$.*

Definition 2.2 (Markov process)**.** *A continuous-time stochastic process $X(t)$ is said to be a Markov process if for any pair of states a, b belonging to a state space $\mathcal{X}$, $X(t)$ has a transition from a to b triggered by an independent Poisson clock with a rate of $q_{ab}(t)$, i.e.*

$$\mathbb{P}[X(t + \Delta t) = b | X(t) = a] = \int_t^{t+\Delta t} q_{ab}(t)\,\mathrm{d}t + o(\Delta t)\,. \tag{2}$$

The transition rate matrix $Q(t) \in \mathbb{R}^{|\mathcal{X}|\times|\mathcal{X}|}$ gathers all transition rates. If Q does not depend on t, then the Markov process is homogeneous; otherwise, it is non-homogeneous.

3. Model

In this section, we present the mathematical model employed to describe the co-evolution of human environmental behaviour and environmental degradation. First, we introduce the network multi-population model. We delineate the division of the population into climate change deniers and acknowledgers and describe how individuals interact with each other. Second, we introduce the dynamical system describing the temporal evolution of the environmental degradation, which depends on human behaviour. Third, we propose a social learning framework describing the evolution of human behaviour. This framework considers several factors, including sensitivity to the environmental state, yielding a feedback loop between the two co-evolving dynamics, as illustrated in Fig. 1.

3.1. Network multi-population model

We consider a population of $n \in \mathbb{Z}_{>0}$ individuals. Each individual $i \in \mathcal{V}$ is characterised by a binary variable $x_i(t) \in \{0, 1\}$, representing the behaviour of the individual at time $t \in \mathbb{R}_{\geq 0}$. Specifically,

$$x_i(t) = \begin{cases} 0 & \text{if } i \text{ has environmentally irresponsible behaviour at time } t, \\ 1 & \text{if } i \text{ behaves responsibly at time } t. \end{cases} \tag{3}$$

The behavioural state of the entire population is captured by gathering all these binary variables in an n-dimensional vector $\mathbf{x}(t) := [x_1(t), x_2(t), \ldots, x_n(t)]^\top \in \{0, 1\}^n$.

Individuals interact on a network structure. Each individual is represented as a vertex in a directed network $\mathcal{G} := (\mathcal{V}, \mathcal{E})$, where $\mathcal{V} := \{1, \ldots, n\}$ and link $(i, j) \in \mathcal{E}$ if and only if (iff) j exerts a social influence on the behaviour of individual i. The set of individuals that influence $i \in \mathcal{V}$ is denoted by $\mathcal{N}_i := \{j \in \mathcal{V} \ : \ (i, j) \in \mathcal{E}\}$. The population is divided into two distinct groups:

1. a subpopulation $\mathcal{D} \subset \mathcal{V}$ of size $n_\mathrm{d} < n$ consisting of climate change *deniers*, who deny that human activities contribute to climate change or even assert that climate change itself is a hoax; and

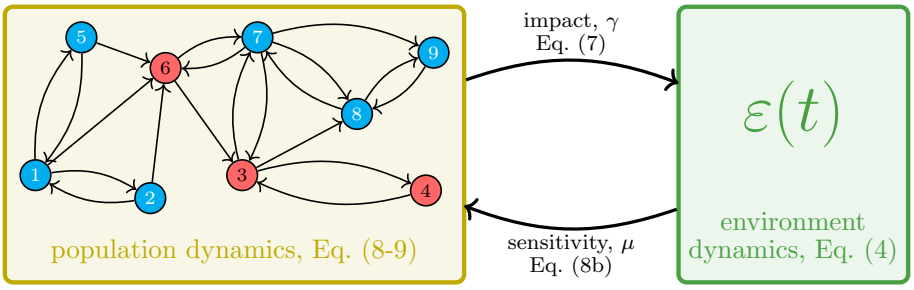

Figure 1: Schematic of the co-evolution of human environmental behaviour and environmental degradation. In this example, the multi-population network has $n = 9$ individuals. Climate change deniers $\mathcal{D} = \{3, 4, 6\}$ are denoted in red, whereas acknowledgers $\mathcal{A} = \{1, 2, 5, 7, 8, 9\}$ are in cyan. Individual 1 is an acknowledger, so $\mathcal{S}_1 = \mathcal{A}$. Individual 1 has three neighbours $\mathcal{N}_1 = \{2, 5, 6\}$ of which two are acknowledgers. Thus, $\mathcal{N}_1 \cap \mathcal{S}_1 = \{2, 5\}$.

2. a subpopulation $\mathcal{A} := \mathcal{V} \setminus \mathcal{D}$ of size $n - n_{\mathrm{d}}$ consisting of individuals who *acknowledge* climate change and are willing to mitigate its impact.

Let $d = \frac{n_{\mathrm{d}}}{n} \in [0, 1)$ denote the fraction of deniers in the population. For any individual $i \in \mathcal{V}$, $\mathcal{S}_i$ denotes the set of individuals that are part of the same subpopulation. For example, if $i \in \mathcal{D}$, then $\mathcal{S}_i = \mathcal{D}$. Fig. 1 illustrates the structure of the population model.

In the rest of the paper, we will make the following assumption.

Assumption 3.1. *The network $\mathcal{G}$ is strongly connected. Moreover, for each $i \in \mathcal{V}$, the set $\mathcal{N}_i \cap \mathcal{S}_i \neq \emptyset$, i.e. each individual has a link with at least one other individual belonging to the same subpopulation.*

Note that Assumption 3.1 is not very restrictive, as it is reasonable to assume that individuals interact with like-minded peers [28, 29, 30, 31] in a highly connected world.

3.2. Environmental degradation

We introduce a scalar variable $\varepsilon(t) \in \mathbb{R}_{\geq 0}$ to represent the level of environmental degradation at time t. In this work, we consider $\varepsilon(t)$ as an abstract variable that captures different aspects associated with environmental degradation,

from pollution and resource depletion to temperature rise. Despite the complexity of all these phenomena—which typically depend on various factors and are often governed by nontrivial (and even unknown) dynamics—observations suggest that many aspects associated with environmental degradation (e.g. CO_2 emissions and extreme weather events) are subject to (at least locally) exponential trends [62, 63, 64]. Consistently, we opt to model the evolution of $\varepsilon(t)$ by means of the following linear, non-autonomous ordinary differential equation (ODE):

$$\dot{\varepsilon} = r(t)\varepsilon. \tag{4}$$

The rate of change $r(t)$ is generally non-constant since it depends on human behaviour. Specifically, we define the macroscopic variables

$$\bar{x}_0(t) := \frac{1}{n}\left|\{i \in \mathcal{V} \ : \ x_i(t) = 0\}\right| \quad \text{and} \quad \bar{x}_1(t) := \frac{1}{n}\left|\{i \in \mathcal{V} \ : \ x_i(t) = 1\}\right| \tag{5}$$

describing the fraction of individuals acting environmentally irresponsibly and responsibly at time t, respectively. Next, we define the rate of change as

$$r(t) := \bar{\gamma}\bar{x}_0(t) + \hat{\gamma}\bar{x}_1(t) - \bar{\tau}, \tag{6}$$

where the coefficients $\bar{\gamma}$ and $\hat{\gamma}$ are the environmental impact of irresponsible and responsible behaviour, respectively, with $\bar{\gamma} > \hat{\gamma} > 0$. Additionally, $\bar{\tau} \in \mathbb{R}_{>0}$ represents endeavours aimed at mitigating the environmental impact, such as large-scale tree-planting initiatives or the deployment of negative emissions technologies. Without any loss in generality, we can simplify Eq. (6) by noting that $\bar{x}_1(t) = 1 - \bar{x}_0(t)$ and by letting $\gamma := \bar{\gamma} - \hat{\gamma}$ and $\tau := \bar{\tau} - \hat{\gamma}$. This yields

$$r(t) := \gamma\bar{x}_0(t) - \tau, \tag{7}$$

where $\gamma \in \mathbb{R}_{>0}$ represents the increased environmental impact of irresponsible behaviour relative to responsible behaviour, and $\tau \in \mathbb{R}_{>0}$ denotes the net efforts in mitigating the environmental impact.

3.3. Human environmental behaviour

Inspired by the decision-making process outlined in [41, 42], we adopt a social learning mechanism inspired by game theory to describe the evolution of

human behaviour. At each time step, each individual decides whether to behave responsibly or irresponsibly based on the values of two utility functions associated with these behaviours. These utility functions, defined in Subsection 3.3.1, capture the incentives that drive individuals to choose a particular behaviour.

3.3.1. Individual's utility functions

Each individual has incentives for environmentally responsible and irresponsible behaviour. These incentives depend on factors such as social influence, the environmental degradation, the presence of awareness campaigns, the relatively higher (economical or social) cost of adopting sustainable behaviour, and governmental subsidies that reduce such a relative cost. For climate deniers ($i \in \mathcal{D}$), the utility function associated with responsible behaviour is solely affected by social influence and is defined by

$$u^{(i)}_{\mathcal{D},1}(\mathbf{x}(t)) := \frac{1}{|\mathcal{N}_i|} \sum_{j \in \mathcal{N}_i} x_j(t)\,. \tag{8a}$$

Eq. (8a) linearly scales with the number of social contacts behaving responsibly, reflecting the influence of peer pressure. Conversely, for any $i \in \mathcal{A}$, we incorporate two additional terms into the utility function to account for acknowledgers' sensitivity to environmental degradation and the presence of awareness campaigns, resulting in the expression

$$u^{(i)}_{\mathcal{A},1}(\mathbf{x}(t), \varepsilon(t)) := \frac{1}{|\mathcal{N}_i|} \sum_{j \in \mathcal{N}_i} x_j(t) + \mu\varepsilon(t) + \alpha\,. \tag{8b}$$

Here, the coefficients $\mu \in \mathbb{R}_{>0}$ and $\alpha \in \mathbb{R}_{\geq 0}$ capture the environmental response and awareness campaigns, respectively, and are extensively described below. Finally, for any individual $i \in \mathcal{V}$, we define the utility function linked to irresponsible behaviour, which considers both social influence and the cost of adopting responsible behaviour, yielding

$$u^{(i)}_{0}(\mathbf{x}(t)) := \frac{1}{|\mathcal{N}_i|} \sum_{j \in \mathcal{N}_i} (1 - x_j(t)) + \kappa\,. \tag{8c}$$

Here, the coefficient $\kappa \in \mathbb{R}_{\geq 0}$ captures net costs associated with acting responsibly, as detailed below. In the subsequent discussion, we discuss the elements that underlie the utility functions presented in Eq. (8).

Social influence. Field experiments provided substantial evidence of the influence of social norms on environmental behaviour [65], e.g. curbside recycling practices [51], towel reuse in hotels [52], and energy-conserving behaviour [53, 54]. The well-established tendency of individuals to conform to their social surroundings [56] is reflected in the first term of Eq. (8a)–Eq. (8c). When more of an individual's neighbours exhibit a particular behaviour, that individual is more likely to engage in the same behaviour.

Environmental sensitivity. For individuals acknowledging climate change ($i \in \mathcal{A}$), the response to this phenomenon and its consequences is modelled by an increased incentive for behaving responsibly, captured by the term $\mu\varepsilon(t)$ in Eq. (8b). Conversely, deniers ($i \in \mathcal{D}$) steadfastly reject either the existence of the climate crisis or dispute the extent of humanity's involvement in its causation. Consequently, such a term is not present in their utility function.

Awareness campaigns. A barrier to the adoption of sustainable behaviour is the lack of available information on how to act responsibly [66]. Awareness campaigns—modelled by the parameter $\alpha \in \mathbb{R}_{\geq 0}$ in Eq. (8b)—boost public knowledge. For individuals acknowledging climate change ($i \in \mathcal{A}$), these campaigns enhance the incentive to engage in responsible behaviour.

Conspiracy theories, which often claim that climate change is a hoax, are strongly associated with alienation from society and distrust in government, scientists, and media [67, 68, 69]. Hence, we assume that awareness campaigns have no effect on the utility functions of deniers ($i \in \mathcal{D}$).

Cost. The higher cost of environmentally friendly behaviour is another barrier to the adoption of responsible behaviour [66, 65]. However, such costs can be reduced by means of government subsidies. The parameter $\kappa \in \mathbb{R}_{>0}$ captures such net costs by amplifying the incentive for irresponsible behaviour in Eq. (8c).

3.3.2. Conformity-driven imitation dynamics

Individuals revise their behaviour based on the utility functions defined in the previous section. Specifically, we assume that behaviour is revised according to a stochastic adaptation of classical *imitation dynamics*, commonly used in social learning [38, 70, 71]. Imitation dynamics is a simple learning protocol based on empirical evidence that imitation of successful strategies is common in both nature and social systems [72, 73]. According to this revision protocol, each individual interacts with their neighbours. Through these interactions, an individual may decide to imitate their neighbour's behaviour, which occurs at a rate proportional to the neighbour's utility. To incorporate homophily—the bias of individuals to imitate those from their own subpopulation [29, 30, 31]—we introduce a parameter $\theta \in (0, 1]$. A higher θ signifies a higher bias towards restricting interactions to like-minded people. If $\theta = 1$, individuals exclusively imitate peers from their own subpopulation. The proposed *conformity-driven imitation dynamics* combines the incentive-driven behavioural tendencies of individuals with their propensity to conform to the behavioural norm of their social environment [56].

Operatively, the human environmental behavioural model can be summarised in the following algorithm:

1. The system is initialised at $t = 0$, with initial conditions $\mathbf{x}(0)$ and $\varepsilon(0)$;

2. Each individual $i \in \mathcal{V}$ is associated with a unit rate Poisson clock, with all clocks being independent of one another and initialised at time t;

3. Until the first clock ticks, the environmental degradation $\varepsilon(t)$ evolves according to Eq. (4) and Eq. (7);

4. Let $i \in \mathcal{V}$ be the first individual whose clock ticks and let t denote the time at which i's clock ticks;

5. Individual i selects one individual ℓ from their neighbours $\mathcal{N}_i := \{j \in \mathcal{V} : (i, j) \in \mathcal{E}\}$. This selection occurs as follows:

(a) with probability θ, i selects a neighbour uniformly at random from those who belong to the same subpopulation as i (i.e. they are selected from $\mathcal{N}_i \cap \mathcal{S}_i$);

(b) otherwise, with probability $1-\theta$, i selects a neighbour uniformly at random from the entire set $\mathcal{N}_i$;

6. With probability proportional to the neighbour's utility—defined in Eq. (8)—individual i imitates the behaviour of ℓ. If this occurs, then i updates their behaviour to $x_i(t^+) = x_\ell(t)$; otherwise, i's behaviour remains unchanged (i.e. $x_i(t^+) = x_i(t^-)$);

7. The algorithm resumes at step 2, starting from time t.

Without any loss of generality, we can re-scale the time variable so that the activation rate of the Poisson clock coincides with the normalisation term of the imitation probability, thus reducing the number of model parameters. According to such dynamics, the behaviour of each individual evolves according to a probabilistic rule, which is derived in the following proposition.

Proposition 3.1. *An individual $i \in \mathcal{V}$ who follows an imitation dynamics with utility functions defined in Eq. (8) and behaves irresponsibly at time t ($x_i(t^-) = 0$) switches to responsible behaviour ($x_i(t^+) = 1$) when triggered by a Poisson clock with a rate of*

$$\rho_{01}^{(i)}(\mathbf{x}(t), \varepsilon(t)) = \theta \frac{1}{|\mathcal{N}_i \cap \mathcal{S}_i|} \sum_{j \in \mathcal{N}_i \cap \mathcal{S}_i} x_j(t) u_{\mathcal{S}_j,1}^{(j)} + (1-\theta) \frac{1}{|\mathcal{N}_i|} \sum_{j \in \mathcal{N}_i} x_j(t) u_{\mathcal{S}_j,1}^{(j)}\,, \tag{9a}$$

whereas an individual $i \in \mathcal{V}$ acting responsibly ($x_i(t^-) = 1$) will cease to do so ($x_i(t^+) = 0$) when triggered by a Poisson clock with a rate of

$$\rho_{10}^{(i)}(\mathbf{x}(t)) = \theta \frac{1}{|\mathcal{N}_i \cap \mathcal{S}_i|} \sum_{j \in \mathcal{N}_i \cap \mathcal{S}_i} \big(1 - x_j(t)\big) u_0^{(j)} + (1-\theta) \frac{1}{|\mathcal{N}_i|} \sum_{j \in \mathcal{N}_i} \big(1 - x_j(t)\big) u_0^{(j)}. \tag{9b}$$

Proof. An individual $i \in \mathcal{V}$ behaving irresponsibly at time t ($x_i(t) = 0$) switches to responsible behaviour when either one of the following two chains of events occurs: i) i activates, decides to interact within their subpopulation, interacts with an individual adopting responsible behaviour, and imitates them; or ii) i activates, decides to interact with someone from the entire population, interacts with an individual adopting responsible behaviour, and imitates them. To compute the rate associated with the first chain of events, we can utilise Proposition 2.1. When individual i activates, i decides to interact within their subpopulation with probability θ; interacts with j with probability $\frac{1}{|\mathcal{N}_i \cap \mathcal{S}_i|}$ since interactions are random; j displays responsible behaviour if $x_j(t) = 1$; and i imitates j proportionally to j's utility function. Using item (ii) of Proposition 2.1, we obtain $\theta \frac{1}{|\mathcal{N}_i \cap \mathcal{S}_i|} x_j(t) u^{(j)}_{\mathcal{S}_j,1}$. By item (i) of Proposition 2.1, summing over all $j \in \mathcal{N}_i \cap \mathcal{S}_i$ yields the first summand in Eq. (9a). Analogously, we compute the rate associated with the second chain of events. We sum the two rates by item (i) of Proposition 2.1. Similarly, we derive Eq. (9b). □

To summarise, the multi-population framework is characterised by the interplay of: i) a collective environment $\varepsilon(t) \in \mathbb{R}_{\geq 0}$, governed by the ODE in Eq. (4) with the rate of change in Eq. (7); and ii) the behavioural state $\mathbf{x}(t)$ of a population consisting of n individuals, evolving according to the revision protocol in Eq. (9), influenced by the behavioural incentives captured in the utility functions in Eq. (8). All the model parameters and variables are summarised in Table 1.

4. Mean-Field Dynamics

Since all behavioural transitions are triggered by Poisson clocks, with each clock independent of the others, the whole behavioural population state $\mathbf{x}(t) \in \{0,1\}^n$ evolves according to an n-dimensional non-homogeneous continuous-time Markov process [57]. Specifically, for any pair of states $\mathbf{x} \in \{0,1\}^n$ and $\hat{\mathbf{x}} \in \{0,1\}^n$ that differ in a single component i (with $x_i = 0$ and $\hat{x}_i = 1$ or vice

Table 1: Model variables and parameters.

symbol	meaning
n	number of individuals
$\mathcal{D}$	subpopulation of climate change deniers
$\mathcal{A}$	subpopulation of climate change acknowledgers
d	fraction of deniers in the population
$\mathcal{N}_i$	neighbours of individual i
$x_i(t)$	behaviour of individual i at time t
$\bar{x}_0(t)$	fraction of population behaving irresponsibly at time t
$\bar{x}_1(t)$	fraction of population behaving responsibly at time t
$\varepsilon(t)$	environmental degradation at time t
γ	increased environmental degradation due to irresponsible behaviour
τ	net endeavours aimed at mitigating environmental degradation
μ	sensitivity to environmental degradation
α	sensitivity to awareness campaigns
κ	net cost for adopting responsible behaviour
θ	homophily

versa), we can write the following non-zero entries of the transition rate matrix:

$$q_{\mathbf{x}\hat{\mathbf{x}}}(t) = \begin{cases} \rho_{01}^{(i)}(\mathbf{x}, \varepsilon(t)) & \text{if } x_i = 0 \text{ and } \hat{x}_i = 1, \\ \rho_{10}^{(i)}(\mathbf{x}) & \text{if } x_i = 1 \text{ and } \hat{x}_i = 0, \end{cases} \tag{10}$$

while all transition rates between states that differ for more than a single component are equal to 0. All entries of the transition rate matrix $Q(\mathbf{x}(t), \varepsilon(t))$—obtained by assembling the rates in Eq. (10)—depend on the behaviour of other individuals through the dependency on the behavioural state of neighbours in Eq. (8) and Eq. (9). Furthermore, the transition rates are non-homogeneous, as some of the rates also depend on $\varepsilon(t)$.

The complexity of the transition rate matrix and the exponential growth of the state space $\{0, 1\}^n$ with population size n make direct analysis of the non-homogeneous Markov process $\mathbf{x}(t)$ infeasible for large-scale populations. Given the exponential increase in analytical complexity with population size n, we adopt a mean-field approach in the limit $n \nearrow \infty$ [58]. This approach, widely used in the study of complex dynamical systems for various applications [42, 74], allows us to reduce the complexity of an n-dimensional Markov process to an n-dimensional set of ODEs that approximate the mean dynamics of the system arbitrarily well as $n \nearrow \infty$ [59, 60].

For any $i \in \mathcal{V}$, we define the probability of behaving responsibly at time t, $p_i(t)$. This probability coincides with the mean dynamics $\mathbb{E}[x_i(t) = 1]$, i.e. $p_i(t) := \mathbb{E}[x_i(t) = 1] = \mathbb{P}[x_i(t) = 1]$. Furthermore, $\mathbb{P}[x_i(t) = 0] = 1 - p_i(t)$.
In order to compute how $p_i(t)$ evolves, we use Definition 2.2 and Eq. (10), yielding

$$\begin{aligned} p_i(t + \Delta t) =& \mathbb{P}[x_i(t + \Delta t) = 1] \\ =& \mathbb{P}[x_i(t + \Delta t) = 1 | x_i(t) = 0] \mathbb{P}[x_i(t) = 0] \\ &+ (1 - \mathbb{P}[x_i(t + \Delta t) = 0 | x_i(t) = 1]) \mathbb{P}[x_i(t) = 1] \\ =& \rho_{01}^{(i)}(\mathbf{x}(t), \varepsilon(t)) \Delta t (1 - p_i(t)) + (1 - \rho_{10}^{(i)}(\mathbf{x}(t)) \Delta t) p_i(t) + o(\Delta t). \end{aligned} \tag{11}$$

By dividing both sides by Δt, taking the limit as $\Delta t \searrow 0$, and re-arranging the

terms, we arrive at

$$\dot{p}_i(t) = \rho_{01}^{(i)}(\mathbf{x}(t), \varepsilon(t))(1 - p_i(t)) - \rho_{10}^{(i)}(\mathbf{x}(t))p_i(t), \tag{12}$$

which is the Chapman-Kolmogorov equation [57] of the Markov process. Interestingly, we observe that although the imitation process seems to depend solely on the utility functions of others, the effective rate at which the probability of adopting responsible behaviours evolves depends in a non-trivial manner on the difference between the payoffs, similar to other (more complicated) revision protocols for social dynamics [75].

Following the procedure proposed in [58], we take the expected value of Eq. (12) on both sides, and use the approximation

$$\mathbb{E}[\rho_{01}^{(i)}(\mathbf{x}(t), \varepsilon(t))] \simeq \rho_{01}^{(i)}(\mathbb{E}[\mathbf{x}(t)], \varepsilon(t)) = \rho_{01}^{(i)}(\mathbf{p}(t), \varepsilon(t)),$$

with $\mathbf{p}(t) := [p_1(t), \ldots, p_n(t)]^\top \in [0,1]^n$, ultimately approximating Eq. (12) with

$$\dot{p}_i(t) = \rho_{01}^{(i)}(\mathbf{p}(t), \varepsilon(t))(1 - p_i(t)) - \rho_{10}^{(i)}(\mathbf{p}(t))p_i(t). \tag{13}$$

While the approximation in Eq. (13) cannot be directly used to predict the behaviour of every single individual, it has proven useful in predicting the emergent behaviour of the system, as detailed below. We define the average probability of behaving responsibly at time t for a randomly chosen $i \in \mathcal{D}$ and $i \in \mathcal{A}$ as

$$y(t) := \frac{1}{nd} \sum_{i \in \mathcal{D}} p_i(t)\,, \quad \text{and} \quad z(t) := \frac{1}{n(1-d)} \sum_{i \in \mathcal{A}} p_i(t)\,, \tag{14}$$

respectively. Hence, the average probability for a randomly selected individual to act responsibly, which we denote as $x(t)$, equals

$$x(t) := \frac{1}{n} \sum_{i \in \mathcal{V}} p_i(t) = dy(t) + (1-d)z(t). \tag{15}$$

For large-scale populations and any finite time horizon, the macroscopic variables $\bar{x}_1(t)$ and $\bar{x}_0(t)$ in Eq. (5) are accurately approximated by means of the average probability $x(t)$ in Eq. (15), i.e. $\bar{x}_1(t) \simeq x(t)$ and $\bar{x}_0(t) \simeq 1 - x(t)$, with approximations becoming exact in the limit $n \nearrow \infty$, as demonstrated in [59, 60], and supported by the numerical simulation in Fig. 2.

In the mean-field framework, the system evolution occurs via an interplay between i) the set of n independent ODEs described in Eq. (13), and ii) the mean-field dynamics of the environmental degradation, obtained by substituting $\bar{x}_0(t)$ with $1 - x(t)$ in Eq. (7). This interplay gives rise to a system of $n + 1$ coupled ODEs, summarised in the following proposition.

Proposition 4.1. *The mean-field evolution of the co-evolutionary system is captured by the following autonomous system of $n + 1$ ODEs:*

$$\dot{p}_i = \rho_{01}^{(i)}(\mathbf{p}, \varepsilon)(1 - p_i) - \rho_{10}^{(i)}(\mathbf{p})p_i \,, \qquad i \in \mathcal{V}, \tag{16a}$$

$$\dot{\varepsilon} = (\gamma(1 - dy - (1 - d)z) - \tau)\varepsilon \,. \tag{16b}$$

While simpler than analysing the original n-dimensional Markov process, directly studying the mean-field dynamics remains challenging due to the inherent complexity of the system of $n + 1$ coupled non-linear ODEs in Eq. (16). To facilitate theoretical analysis, we introduce the following simplifying assumption stating that each individual can interact with all others, i.e. that individuals interact on a complete network.

Assumption 4.1. *Any individual $i \in \mathcal{V}$ is influenced by the entire population, i.e. $\mathcal{N}_i = \mathcal{V}$ for all $i \in \mathcal{V}$.*

Under Assumption 4.1, we further simplify the mean-field dynamics by deriving a lower-dimensional set of ODEs describing the temporal evolution of the macroscopic variables in Eq. (14), which ultimately describe the emergent system behaviour.

Proposition 4.2. *Under Assumption 4.1 and in the limit of large-scale populations $n \to \infty$, the mean-field evolution of the macroscopic behavioural states y, z and the environmental degradation ε is governed by the following three-dimensional autonomous system of ODEs:*

$$\begin{aligned}\dot{y} =& \Big((\theta + d(1 - \theta))(dy + (1 - d)z)y\Big)(1 - y) \\ &+ \Big((1 - d)(1 - \theta)(dy + (1 - d)z + \mu\varepsilon + \alpha)z\Big)(1 - y)\end{aligned}$$

$$-\Big(1-dy-(1-d)z+\kappa\Big)\Big(1-(\theta+d(1-\theta))y-(1-d)(1-\theta)z\Big)y\,, \quad (17a)$$

$$\dot{z}=\Big((1-d(1-\theta))(dy+(1-d)z+\mu\varepsilon+\alpha)z+d(1-\theta)(dy+(1-d)z)y\Big)\cdot$$
$$\cdot(1-z)-\Big(1-dy-(1-d)z+\kappa\Big)\Big(1-d(1-\theta)y-(1-d(1-\theta))z\Big)z\,, \quad (17b)$$

$$\dot{\varepsilon}=(\gamma(1-dy-(1-d)z)-\tau)\varepsilon\,. \quad (17c)$$

Proof. Under Assumption 4.1, we observe that in the mean-field framework, the utility functions in Eq. (8) simplify to expressions that are independent of i and depend on $\mathbf{p}$ solely through the macroscopic variables y and z:

$$u^{(i)}_{\mathcal{D},1}(\mathbf{p})=\frac{1}{n}\sum_{j\in\mathcal{V}}p_j=x=dy+(1-d)z\,, \quad (18a)$$

$$u^{(i)}_{\mathcal{A},1}(\mathbf{p},\varepsilon)=\frac{1}{n}\sum_{j\in\mathcal{V}}p_j+\mu\varepsilon+\alpha=x+\mu\varepsilon+\alpha=dy+(1-d)z+\mu\varepsilon+\alpha\,, \quad (18b)$$

$$u^{(i)}_{0}(\mathbf{p})=\frac{1}{n}\sum_{j\in\mathcal{V}}(1-p_j)+\kappa=1-x+\kappa=1-dy-(1-d)z+\kappa\,. \quad (18c)$$

By substituting the expressions in Eq. (18) into Eq. (9), we obtain

$$\rho^{(i)}_{01}(\mathbf{p},\varepsilon)=(\theta+d(1-\theta))(dy+(1-d)z)y$$
$$+(1-d)(1-\theta)(dy+(1-d)z+\mu\varepsilon+\alpha)z\,, \quad (19a)$$

$$\rho^{(i)}_{10}(\mathbf{p})=\big(1-dy-(1-d)z+\kappa\big)\big(1-(\theta+d(1-\theta))y-(1-d)(1-\theta)z\big)\,, \quad (19b)$$

for any $i\in\mathcal{D}$, and

$$\rho^{(i)}_{01}(\mathbf{p},\varepsilon)=\big(1-d(1-\theta)\big)\big(dy+(1-d)z+\mu\varepsilon+\alpha\big)z+d(1-\theta)\big(dy+(1-d)z\big)y\,, \quad (19c)$$

$$\rho^{(i)}_{10}(\mathbf{p})=\big(1-dy-(1-d)z+\kappa\big)\big(1-d(1-\theta)y-(1-d(1-\theta))z\big)\,, \quad (19d)$$

for any $i\in\mathcal{A}$. Finally, by substituting Eq. (19) into Eq. (13) and noting that the linearity of the derivative operator implies

$$\dot{y}(t):=\frac{1}{nd}\sum_{i\in\mathcal{D}}\dot{p}_i\,,\qquad \dot{z}(t):=\frac{1}{n(1-d)}\sum_{i\in\mathcal{A}}\dot{p}_i\,, \quad (20)$$

we obtain the system in Eq. (17). □

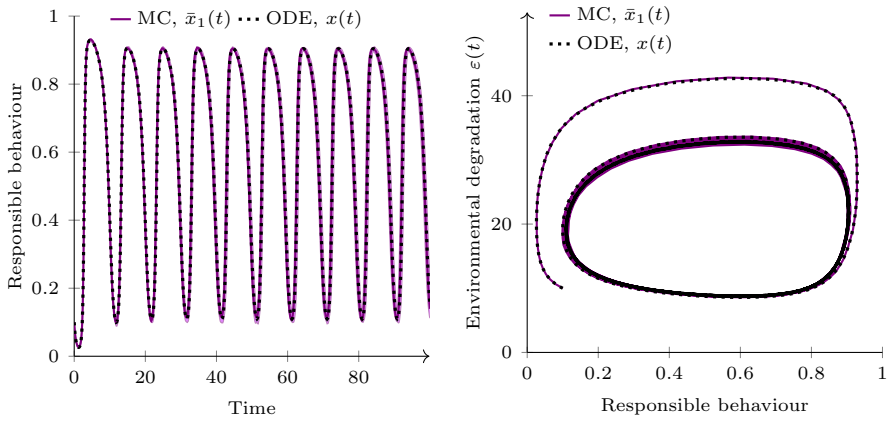

(a) Temporal evolution

(b) State-space

Figure 2: Comparison between the average of 100 independent simulations of a Markov chain (violet, solid) and its mean-field approximation (black, dotted) for $n = 100\,000$. The violet region in panel (a) represents the envelope of 100 independent simulations. Parameters are $\theta = 0.8$, $d = 0.15$, $\alpha = 0.1$, $\kappa = 3.5$, $\gamma = 1$, $\tau = 0.4$, and $\mu = 0.2$.

Fig. 2 compares an ensemble of trajectories of the Markov chain (with transition rates defined in Eq. (10)) with its mean-field approximation (derived using Proposition 4.2). In particular, the comparison confirms that the variable $x(t)$—obtained by integrating the system of ODEs in the mean-field approximation—serves as a good proxy for the quantity $\bar{x}_1(t)$ for sufficiently large populations (in these simulations, we set $n = 100\,000$). Interestingly, the simulations show a precise match, both in terms of the temporal trajectory and the trajectory on the state-space, with the average discrepancy between $\bar{x}_1(t)$ and $x(t)$ over 100 independent simulations of the Markov chain being less than 1%. Consistent results have been obtained for different sets of parameter values. This close agreement between the Markov chain and its mean-field approximation suggests that analysing the system of ODEs in Eq. (17) can offer valuable insights into the emergent behaviour of the stochastic behavioural–environmental model, particularly for large-scale populations.

Remark 4.1. *In the limit case $d = 0$, for which deniers are not present in the*

population, the system in Eq. (17) reduces to the single-population model with equations

$$\dot{x} = x(1-x)(2x + \mu\varepsilon + \alpha - \kappa - 1)\,, \tag{21a}$$

$$\dot{\varepsilon} = (\gamma(1-x) - \tau)\varepsilon\,, \tag{21b}$$

which was introduced and studied in [55].

In the rest of this paper, we will focus on the scenario $d > 0$, i.e. when deniers are present, and we will investigate how their presence affects the emergent behaviour of the population and, ultimately, environmental degradation.

5. Main Results

Before proceeding with the analysis of the asymptotic behaviour of the dynamical system derived in Proposition 4.2, we introduce some additional realistic assumptions that ensure the well-posedness of the system in Eq. (17). First, we assume that the environment deteriorates if the entire population behaves irresponsibly. This assumption, which relies on scientific evidence of the impact of human activity on climate change [2, 3, 17, 4, 7, 18], is modelled by imposing that $\dot{\varepsilon} > 0$ when $y = z = 0$, which holds iff $\tau < \gamma$. Second, we assume that in the absence of any environmental degradation (i.e. for $\varepsilon = 0$), there is no incentive to prefer responsible over irresponsible behaviour, i.e. $u_0^{(i)}(\mathbf{p}) > u_{\mathcal{S}_i,1}^{(i)}(\mathbf{p}, 0)$ for any $i \in \mathcal{V}$ and any $\mathbf{p} \in [0,1]^n$. This holds iff $\kappa > \alpha + 1$. Third, climate change deniers are (fortunately) a minority [20]. Here, we focus on the scenario in which the fraction of climate deniers is small enough for the environmental degradation to decrease if all climate change acknowledgers $i \in \mathcal{A}$ act responsibly, regardless of the behaviour of the deniers. In other words, if $z = 1$, then we impose that $\dot{\varepsilon} < 0$ for any $y \in [0,1]$, which is attained iff $d < \tau/\gamma$. Fourth, we assume that deniers are present (the case $d = 0$ reduces to the model treated in [55]). In summary, these conditions directly lead to the following constraints on the model parameters.

Assumption 5.1. *We assume that (i) $\tau < \gamma$; (ii) $\kappa > \alpha + 1$; (iii) $d < \tau/\gamma$; and (iv) $d > 0$.*

Looking back at environmental population behaviour and carbon dioxide emissions over the past 50 years [62, 63], there was a massive display of irresponsible behaviour during the initial phase when the environmental degradation began to rise. We consider a scenario that begins when the environmental degradation is a cause for concern (i.e. $\varepsilon(0) > 0$) and when some level of responsible behaviour is present—at least among acknowledgers ($z(0) > 0$). Thus, we assume that $y(0)$, $z(0)$, and $\varepsilon(0)$ satisfy the following set of conditions.

Assumption 5.2. *The initial conditions of the dynamical system in Eq. (17) satisfy $(y(0), z(0), \varepsilon(0)) \in [0, 1) \times (0, 1) \times \mathbb{R}_{>0}$.*

Remark 5.1. *The limit case $\varepsilon(0) = 0$ can be easily treated analytically, as the system's evolution would be constrained on the plane $\varepsilon = 0$ (since $\varepsilon = 0$ is always an equilibrium for Eq. (17c)), yielding a heterogeneous imitation dynamics for a coordination game where action 0 is always favoured (since $u_0^{(i)}(\mathbf{p}) > u_{\mathcal{S}_i,1}^{(i)}(\mathbf{p}, 0)$ due to item (ii) of Assumption 5.1). Consequently, the system would always converge to the equilibrium $(0, 0, 0)$. However, this limit case is not relevant to our study, as it considers a scenario with no environmental degradation.*

Under the reasonable assumptions outlined above, we can rigorously prove both the well-definedness of the dynamical system and the invariance of its domain.

Proposition 5.1. *Consider the mean-field system in Eq. (17) under Assumptions 5.1 and 5.2. Then, there exists an upper bound $\bar{\varepsilon} \in \mathbb{R}_{>0}$ such that $\varepsilon(t) \leq \bar{\varepsilon}$ for all $t \in \mathbb{R}_{\geq 0}$. Additionally, the dynamics in Eq. (17) are well-defined in the sense that $(y(t), z(t), \varepsilon(t)) \in [0, 1] \times [0, 1] \times \mathbb{R}_{\geq 0}$ for all $t \in \mathbb{R}_{\geq 0}$.*

Proof. The proof is reported in Appendix A. □

This technical result guarantees that the mean-field system in Eq. (17) is well-defined, meaning that the variables remain bounded within their domains.

Additionally, Proposition 5.1 ensures that the mean-field system has good mathematical properties such as Lipschitz-continuity, ensuring the existence of its solution. These properties allow us to study the system using analytical tools and numerical solvers, as we demonstrate in the following subsections.

5.1. Complete homophily

Due to the complexity of the system in Eq. (17), computing its equilibria and assessing their stability is a nontrivial task. Therefore, we will start our analysis by considering the scenario where individuals have a complete bias for their subpopulation—that is, we consider the mean-field system in Eq. (17) for $\theta = 1$, for which the dynamics simplify to the equations summarised in the following proposition.

Proposition 5.2 (Complete homophily)**.** *Let $\theta = 1$. Under Assumption 4.1 and in the limit of large-scale populations $n \to \infty$, the mean-field evolution of the macroscopic behavioural states y, z and the environmental degradation ε is governed by the following autonomous system:*

$$\dot{y} = y(1-y)(2(dy + (1-d)z) - \kappa - 1)\,, \tag{22a}$$

$$\dot{z} = z(1-z)(2(dy + (1-d)z) + \mu\varepsilon + \alpha - \kappa - 1)\,, \tag{22b}$$

$$\dot{\varepsilon} = (\gamma(1 - dy - (1-d)z) - \tau)\varepsilon\,. \tag{22c}$$

In the rest of this subsection, we perform a theoretical analysis of the multi-population system with complete homophily in Eq. (22), whose equations directly follow from Proposition 17. The system in Eq. (22) is well-defined, as guaranteed by Proposition 5.1. Moreover, in this scenario of complete homophily, we can refine the results in Proposition 5.1, demonstrating that if the initial conditions lie in the domain specified in Assumption 5.2, the trajectory will remain in that domain without reaching the boundaries $y = 1$, $z = 0$, $z = 1$, and $\varepsilon = 0$.

Proposition 5.3. *Consider the mean-field system with complete homophily ($\theta = 1$) in Eq. (22) under Assumptions 5.1 and 5.2. Then, in addition to the*

results of Proposition 5.1, it holds true that $(y(t), z(t), \varepsilon(t)) \in [0,1) \times (0,1) \times \mathbb{R}_{>0}$ *for all* $t \in \mathbb{R}_{\geq 0}$.

Proof. The proof is reported in Appendix B. □

Under the initial conditions specified in Assumption 5.2, we demonstrate that the mean-field system with complete homophily presented in Eq. (22) has a unique equilibrium, which we analytically compute. Furthermore, we analyse the stability properties of this equilibrium and derive the following result.

Proposition 5.4. *Under Assumptions 5.1 and 5.2, the mean-field system with complete homophily* ($\theta = 1$) *in Eq. (22) has a unique equilibrium in the invariant domain* $[0,1) \times (0,1) \times \mathbb{R}_{>0}$*, which is the following point:*

$$(\bar{y}, \bar{z}, \bar{\varepsilon}) \quad = \left(0,\ \tfrac{1}{1-d}\left(1 - \tfrac{\tau}{\gamma}\right),\ \tfrac{1}{\mu}\left(\tfrac{2\tau}{\gamma} + \kappa - \alpha - 1\right)\right). \tag{23}$$

This equilibrium is a repelling saddle point.

Proof. The proof is presented in Appendix C. □

Remark 5.2. *Recall that the average probability for a randomly selected individual to act responsibly is given by* $x(t) = dy(t) + (1-d)z(t)$*. Therefore, for the unique equilibrium in Eq. (23), we have that*

$$\bar{x} := d\bar{y} + (1-d)\bar{z} = 1 - \tfrac{\tau}{\gamma}, \tag{24}$$

which combined with $\bar{\varepsilon}$ *coincides with the unique interior equilibrium of the single-population system introduced in [55].*

Building on Proposition 5.4, we fully characterise the asymptotic behaviour of the system by establishing the following (almost) global convergence result.

Theorem 5.1. *Consider the mean-field system with complete homophily* ($\theta = 1$) *in Eq. (22) under Assumptions 5.1 and 5.2. If the initial condition does not coincide with the unique equilibrium in Eq. (23), then the system converges to a periodic solution.*

Proof. Consider $(y, z, \varepsilon) \in [0, 1) \times (0, 1) \times \mathbb{R}_{>0}$. By Proposition 5.4, the unique equilibrium is a repelling saddle point with inflow along the y-axis. As $\dot{y} < 0$ for $y \in (0, 1)$, y will converge exponentially to 0. Hence, the system in Eq. (22) is a transient perturbation of the planar system obtained by setting $y = 0$, which is given by

$$\dot{z} = z(1 - z)(2(1 - d)z + \mu\varepsilon + \alpha - \kappa - 1)\,, \tag{25a}$$

$$\dot{\varepsilon} = (\gamma(1 - (1 - d)z) - \tau)\varepsilon\,. \tag{25b}$$

Let us consider the planar system in Eq. (25). By Proposition 5.3, $(z(t), \varepsilon(t)) \in (0, 1) \times \mathbb{R}_{>0}$ for all $t \in \mathbb{R}_{\geq 0}$ if $(z(0), \varepsilon(0)) \in (0, 1) \times \mathbb{R}_{>0}$. Furthermore, the environmental degradation $\varepsilon(t)$ is bounded from above by Proposition 5.1. Since the equilibrium in Eq. (23) is unstable in the $z\varepsilon$-plane, no homoclinic orbit exists. It follows from the Poincaré-Bendixson theorem [61] that every non-empty compact ω-limit set of an orbit is periodic. □

Theorem 5.1 demonstrates that, for nearly all initial conditions, the trajectories of the coupled behavioural–environmental system exhibit sustained oscillations. These trajectories oscillate around a repelling saddle point, characterised in Eq. (23). Interestingly, the environmental degradation in this unstable equilibrium is independent of the fraction of deniers d, but it does depend on the other behavioural parameters. Specifically, the equilibrium degradation $\bar{\varepsilon}$ increases with a higher net cost for adopting responsible behaviour κ, whereas it decreases with higher sensitivity to degradation μ and awareness campaigns α. Furthermore, we observe from Eq. (25a) that there exists a critical level of environmental degradation $\varepsilon^* = \frac{\kappa+1-\alpha}{\mu}$ above which individuals start adopting environmentally responsible behaviour (i.e. $\dot{z} > 0$), regardless of the social influence mechanism, which may reduce this critical threshold. For a visualisation of this evolution, we refer to the simulations in [55], which are obtained in the special case where $d = 0$. It is also worth noting that even though the fraction of deniers does not impact the repelling saddle point around which trajectories oscillate, it is evident from Eq. (25b) that the environmental degradation starts

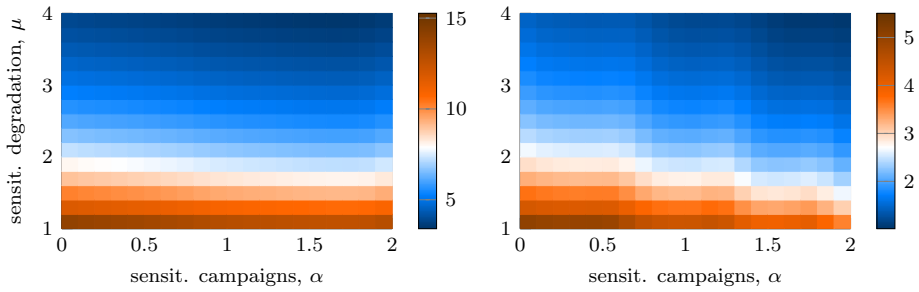

(a) Maximum degradation

(b) Average degradation

Figure 3: Results of numerical integration of Eq. (22), varying the sensitivity to environmental degradation μ and awareness campaigns α. In (a), we report the maximum level of environmental degradation during the simulation using a colour code; in (b) its average value. Common parameters are $d = 0.2$, $\gamma = 1$, $\tau = 0.8$, and $\kappa = 4$. Each data point is obtained as the average of 100 independent simulations with randomised initial conditions.

decreasing when the fraction of adopters of sustainable behaviours exceeds a certain threshold, i.e $z > \frac{\gamma-\tau}{\gamma(1-d)}$. This threshold increases as the fraction of deniers increases, implying that higher fractions of deniers lead to larger oscillations in environmental degradation. An extensive analysis of the role of deniers will be performed in the next section by means of numerical simulations, to corroborate and extend our analytical insights. In summary, these observations highlight the impact of the decision-making parameters μ, α, and κ on the maximum level of environmental degradation, as well as the impact of the fraction of deniers d on the average and peak environmental degradation during periodic oscillations.

The role of the sensitivity to degradation μ and awareness campaigns α is explored in Fig. 3, where we numerically integrate Eq. (22) and evaluate the maximum level of environmental degradation and its mean value, for trajectories obtained with varying values of sensitivity to environmental degradation μ and awareness campaigns α. Predictably, the numerical simulations—where each data point is averaged over 100 independent samplings with initial conditions picked uniformly at random from $[0, 1] \times [0, 1] \times [0, 1]$—suggest that μ

plays a key role in determining the emergent system behaviour both in terms of the maximum and average environmental degradation. Specifically, if μ becomes too small, the maximum environmental degradation increases drastically. Conversely, increasing the sensitivity to awareness campaigns α is important in reducing the average value, but its impact on the maximum environmental degradation is only marginal. These findings underscore the importance of enhancing human sensitivity to environmental degradation by highlighting the ongoing climate change and the escalating environmental degradation, towards fostering a collective response.

5.2. Partial homophily

The results in Section 5.1 suggest that, under some reasonable assumptions, the system approaches a periodic solution in the presence of complete homophily ($\theta = 1$). The regularity of the system in Eq. (17) with respect to the parameter θ combined with the fact that the saddle point in Eq. (23) and the periodic solution found in Theorem 5.1 are hyperbolic allow us to leverage standard regular perturbation arguments [76] to claim that the results proved in Theorem 5.1 also persist for partial homophily, when θ is large but less than 1. However, the complexity of the system in Eq. (17) poses challenges for theoretical analysis in such a general case. Nevertheless, the derivation of the mean-field equations in Proposition 4.2 offers a fast and effective simulation tool to perform numerical campaigns towards exploring the impact of partial homophily on the system. The low dimensionality and deterministic nature of the mean-field dynamics for the macroscopic variables allow for simulating the system's asymptotic behaviour by numerically integrating the 3-dimensional system of nonlinear ODEs using standard numerical solvers (the code used for our simulations is publicly available at `https://github.com/lzino90/bem`).

We start our campaign of numerical simulations by presenting a single trajectory of the dynamical system, illustrated in Fig. 4. This simulation reveals that periodic oscillations are also present in the mean-field system with partial homophily, suggesting that convergence to a periodic solution—analytically

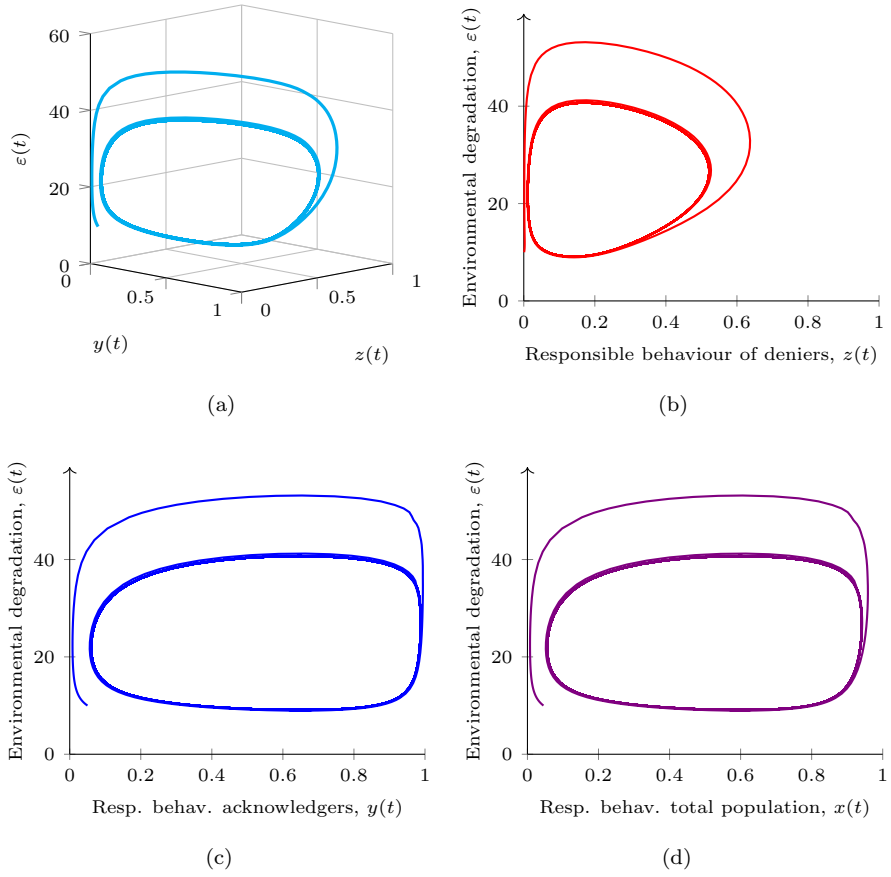

Figure 4: Representative trajectory of the system in Eq. (17). In (a), we report the trajectory in the 3-dimensional space. Additionally, we show three projections with on the x-axis the fraction of responsible behaviour for: (b) climate change deniers y; (c) acknowledgers z; and (d) the total population $x = dy + (1-d)z$. Parameters are $\theta = 0.8$, $d = 0.15$, $\alpha = 0.1$, $\kappa = 3.5$, $\gamma = 1$, $\tau = 0.4$, and $\mu = 0.2$.

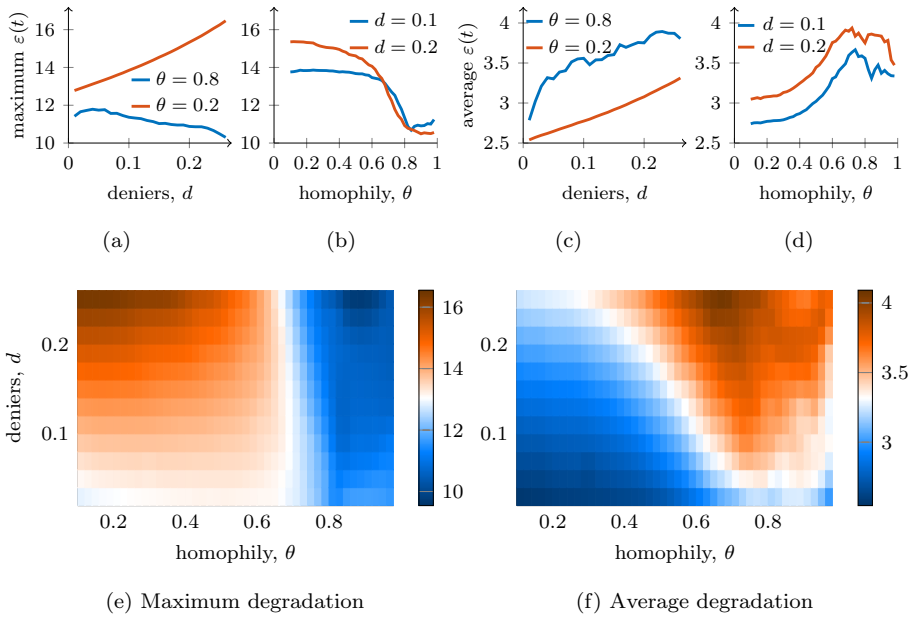

Figure 5: Results of numerical integration of Eq. (17), varying the fraction of deniers d and the level of homophily θ. In (a,b,e), we report the maximum environmental degradation during the simulation; in (c,d,f) its average value. Common parameters are $\kappa = 2$, $\mu = 1$, $\gamma = 1$, $\tau = 0.8$, and $\alpha = 0$. Each data-point is obtained as the average of 100 independent simulations with randomised initial conditions within the domain.

proven in Theorem 5.1 for the limit case $\theta = 1$—is a general characteristic of the co-evolutionary model. To observe the temporal evolution of both climate change deniers and acknowledgers, Figs. 4b and 4c display projections of the trajectory in Fig. 4a on the $y\varepsilon$-plane and the $z\varepsilon$-plane, respectively. Fig. 4d depicts the average behaviour of the entire population, x. These plots highlight the emergence of cyclic oscillations in both human behaviour and the environmental degradation.

The results of our numerical simulation reported in Fig. 4 (supported by additional simulations performed with varied parameter values and initial conditions) suggest that partial homophily does not affect the emergent behaviour of the system from a qualitative standpoint, as all trajectories show oscillating

behaviour. However, the level of homophily may have a non-negligible quantitative impact on the system. In what follows, we present a campaign of numerical simulations to explore this research question further.

Specifically, we numerically integrate Eq. (17) for varying values of homophily (θ) and fractions of deniers (d) while keeping all the other parameters fixed. In all simulations, we consistently observe convergence of the system to a periodic solution. To quantitatively assess the environmental impact of the fraction of deniers and the level of homophily, we evaluate the maximum value and the mean value of the environmental degradation over these simulations, averaging the results over 100 independent realisations of initial conditions sampled uniformly at random within the range $(y(0), z(0), \varepsilon(0)) \in [0,1] \times [0,1] \times [0,5]$, and simulated over a long time-horizon of duration $T = 10\,000$, so that the trajectories approach their asymptotic behaviour.

Our results, reported in Fig. 5, reveal non-trivial behaviour. Specifically, Fig. 5a suggests that the presence of a minority of climate change deniers may—in a counter-intuitive fashion—decrease the maximal value of $\varepsilon(t)$ reached during simulations. In particular, this is observed when the level of homophily is high (blue curve in Fig. 5a), suggesting that the majority of climate change acknowledgers can quickly react when the environmental degradation gets worse by marginalising the minority of deniers. However, a similar counter-intuitive phenomenon is not observed when considering the average value of $\varepsilon(t)$, for which increasing the number of deniers is always detrimental (see Fig. 5c). Even a small minority of deniers can result in dramatic increases in the average environmental degradation, especially in highly polarised scenarios. For instance, by increasing the fraction of deniers from 1% to 4%, the average environmental degradation worsens by more than 20%.

Furthermore, homophily also has a non-trivial impact on the system. In general, increasing the level of homophily seems to yield beneficial effects on the maximal environmental impact (see Fig. 5b). This observation suggests that marginalising the minority of climate change deniers could be a potential strategy to prevent extreme environmental degradation. However, Fig. 5d

shows that highly polarised populations seem to yield worse average values of environmental degradation. This finding suggests that while marginalising deniers effectively curbs peak values, it comes at the cost of worsening the average value, yielding a non-trivial trade-off problem. These preliminary observations are confirmed by a systematic study (reported in Figs. 5e and 5f), in which we compute the maximal and mean values of the environmental degradation for all possible configurations of the parameters θ and d.

6. Conclusion

In this paper, we considered a multi-population modelling framework that accounts for climate change deniers and polarised public opinion. The model incorporated factors such as social influence, policy interventions, negative emission technologies, and the relatively higher costs associated with environmentally friendly behaviour. Individuals revised their behaviour based on a decision-making mechanism where they imitated those with higher behavioural incentives while conforming to social behavioural norms.

We employed a mean-field approach to analyse the emergent behaviour of the system in the limit of large-scale populations. Under complete homophily—where individuals exclusively imitate like-minded peers—we performed a theoretical analysis of the mean-field system and identified the unique equilibrium. We demonstrated that the multi-population behavioural–environmental model converges to a periodic solution for nearly all initial conditions. Numerical simulations support these findings, suggesting the existence of periodic behaviour also for scenarios with incomplete homophily. Additionally, simulations shed light on the non-trivial impact of partial homophily and the fraction of climate change deniers present in the population on the maximum level of environmental degradation and its average value. Counter-intuitively, under the assumptions of our model, it seems that the presence of a minority of deniers is beneficial in mitigating the most extreme consequences of climate change. For highly polarised scenarios—when deniers are marginalised by the rest of the population—climate

change acknowledgers may react more quickly to environmental deterioration, leading to smaller oscillations. However, our numerical simulations also show that even a small minority of deniers leads to a drastic increase in the average environmental degradation during oscillations. These results could support policymakers in making informed decisions to combat climate change. In particular, after calibrating the model to real-world data, the model can be used to explore a wide range of what-if scenarios involving different types of interventions—such as increasing individuals' sensitivity to environmental degradation or implementing awareness campaigns—which can be mapped to parameters of our model.

It is important to mention that our study is not exempt from limitations, which should be carefully considered before utilising our results in real-world scenarios. First, our analytical results are limited to the scenario of perfect homophily and all-to-all communication. Expanding the theoretical treatment to incomplete homophily (so far only treated numerically) and complex social network interactions is crucial to enhance the model's applicability to real-world scenarios. For the latter, refined implementations of mean-field dynamics may be derived, e.g. by following the approaches proposed in the recent complex systems literature [77, 78]. Second, our model considered two subpopulations: climate change acknowledgers and deniers. However, a 2021 global survey with 1.2 million respondents [79] stated that among those recognising climate change as a global emergency, 59% advocated for immediate and urgent action, 20% said we should act slowly, and 10% believed that the world is currently taking sufficient measures. Our framework is readily adaptable to include additional subpopulations, e.g. fast- and slow-responding individuals, by assigning them distinct coefficients of environmental sensitivity. Third, all terms and mechanisms in our mathematical framework are grounded in social psychology and behavioural theory and/or supported by empirical evidence. However, a thorough validation of the mathematical model using existing behavioural data and controlled laboratory experiments and further studies using different revision protocols [75] should be performed before the model can be employed to inform

governmental actions. Fourth, when applying the model to specific aspects of environmental degradation, one may consider refining the environmental dynamics by encapsulating further elements tailored to the problem under investigation.

Finally, in this paper, we assumed that governmental efforts are constant. In reality, such efforts evolve on the basis of public opinion and the severity of the climate change crisis. Effectively addressing climate change requires policies that, for example, ensure meat prices reflect their environmental costs [16, 14]. However, governments currently heavily subsidise the meat industry [80], impeding a shift towards healthier, plant-based diets. Similarly, airlines benefit from exemptions on kerosene tax and VAT on international flights, creating substantial price differences between air and rail travel tickets. Despite flying having over 80 times the climate impact of train travel, train tickets are about twice as expensive on average [81]. Fortunately, the European Parliament is shifting towards more actively subsidising sustainable sectors, adopting policies that support an environmentally friendly food system [82], and planning to end all fossil fuel subsidies [83]. In future research, we plan to incorporate a non-trivial control action into our mathematical model, thereby obtaining an optimisation framework that can support public authorities and decision-makers in planning effective interventions and policy efforts. To this aim, we will leverage the mathematical theory of systems and controls, which has proven successful in mitigating crises such as the COVID-19 pandemic [84, 85, 86].

CRediT authorship contribution statement

Kathinka Frieswijk: Conceptualisation, Methodology, Formal analysis, Funding acquisition, Investigation, Software, Validation, Visualisation, Writing — Original Draft

Lorenzo Zino: Conceptualisation, Methodology, Investigation, Software, Visualisation, Writing — Review & Editing, Supervision

A. Stephen Morse: Funding acquisition, Supervision, Writing — Review & Editing

Ming Cao: Funding acquisition, Supervision, Project administration, Writing — Review & Editing

Declaration of Competing Interest

The authors declare that they have no known competing financial interests or personal relationships that could have appeared to influence the work reported in this paper.

Acknowledgments

The work of M. Cao was supported in part by the Netherlands Organization for Scientific Research, under grant number NWO-Vici-19902. The work of A.S. Morse was supported in part by the Air Force Office of Scientific Research, under grant number FA9550-23-1-0175. The work of K. Frieswijk was supported in part by the Stichting Fulbright Commission the Netherlands, the Hendrik Mullerfonds, and the Stichting het Scholten–Cordes Fonds. The authors thank Ji Liu for discussion.

Data statement

The article has no additional data. The code used for the numerical simulations is available at `https://github.com/lzino90/bem`.

References

[1] IPCC, Climate change 2021: The physical science basis. contribution of Working Group I to the Sixth Assessment Report of the Intergovernmental Panel on Climate Change (2021). doi:10.1017/9781009157896.

[2] NASA, Global climate change: Vital signs of the planet, available at `http://climate.nasa.gov` (2024).

[3] Word Meteorological Organization, Provisional state of the global climate 2023, available at https://wmo.int/files/provisional-state-of-global-climate-2023 (10 2023).

[4] IPCC, Climate change 2023: Synthesis report, available at https://report.ipcc.ch/ar6syr/pdf/IPCC_AR6_SYR_LongerReport.pdf (2023).

[5] I. M. Otto, J. F. Donges, R. Cremades, A. Bhowmik, R. J. Hewitt, W. Lucht, J. Rockström, F. Allerberger, M. McCaffrey, S. S. P. Doe, A. Lenferna, N. Morán, D. P. van Vuuren, H. J. Schellnhuber, Social tipping dynamics for stabilizing Earth's climate by 2050, Proceedings of the National Academy of Sciences 117 (5) (2020) 2354–2365. doi:10.1073/pnas.1900577117.

[6] United Nations Framework Convention on Climate Change, Paris Agreement, available at https://unfccc.int/sites/default/files/resource/parisagreement_publication.pdf (12 2015).

[7] IPCC, Global warming of 1.5°C, available at https://www.ipcc.ch/sr15/ (2018).

[8] Copernicus Climate Change Service, Climate Bulletin March: March 2024 is the tenth month in a row to be the hottest on record, available at https://climate.copernicus.eu/copernicus-march-2024-tenth-month-row-be-hottest-record (2024).

[9] IPCC, Climate change 2022: impacts, adaptation and vulnerability, available at https://www.ipcc.ch/report/sixth-assessment-report-working-group-ii (2022).

[10] E. G. Hertwich, G. P. Peters, Carbon footprint of nations: a global, trade-linked analysis, Environmental Science & Technology 43 (16) (2009) 6414–6420. doi:10.1021/es803496a.

[11] G. Dubois, B. Sovacool, C. Aall, M. Nilsson, C. Barbier, A. Herrmann, S. Bruyère, C. Andersson, B. Skold, F. Nadaud, F. Dorner, K. R. Moberg,

J. P. Ceron, H. Fischer, D. Amelung, M. Baltruszewicz, J. Fischer, F. Benevise, V. R. Louis, R. Sauerborn, It starts at home? Climate policies targeting household consumption and behavioral decisions are key to low-carbon futures, Energy Research & Social Science 52 (2019) 144–158. doi:10.1016/j.erss.2019.02.001.

[12] International Energy Agency, Commentary: As their sales continue to rise, SUVs' global CO_2 emissions are nearing 1 billion tonnes, last accessed: April 7, 2025; available at `https://www.iea.org/commentaries/as-their-sales-continue-to-rise-suvs-global-co2-emissions-are-nearing-1-billion-tonnes` (2023).

[13] M. Crippa, E. Solazzo, D. Guizzardi, F. Monforti-Ferrario, F. N. Tubiello, A. Leip, Food systems are responsible for a third of global anthropogenic GHG emissions, Nature Food 2 (3) (2021) 198–209. doi:10.1038/s43016-021-00225-9.

[14] X. Xu, P. Sharma, S. Shu, T.-S. Lin, P. Ciais, F. N. Tubiello, P. Smith, N. Campbell, A. K. Jain, Global greenhouse gas emissions from animal-based foods are twice those of plant-based foods, Nature Food 2 (9) (2021) 724–732. doi:10.1038/s43016-021-00358-x.

[15] M. Springmann, M. Clark, D. Mason-D'Croz, K. Wiebe, B. L. Bodirsky, L. Lassaletta, W. de Vries, S. J. Vermeulen, M. Herrero, K. M. Carlson, M. Jonell, M. Troell, F. DeClerck, L. J. Gordon, R. Zurayk, P. Scarborough, M. Rayner, B. Loken, J. Fanzo, H. C. J. Godfray, D. Tilman, J. Rockström, W. Willett, Options for keeping the food system within environmental limits, Nature 562 (7728) (2018) 519–525. doi:10.1038/s41586-018-0594-0.

[16] J. Poore, T. Nemecek, Reducing food's environmental impacts through producers and consumers, Science 360 (6392) (2018) 987–992. doi:10.1126/science.aaq0216.

[17] A. L. Westerling, Increasing western US forest wildfire activity: sensitivity to changes in the timing of spring, Philosophical Transactions

of the Royal Society B: Biological Sciences 371 (1696) (2016) 20150178. doi:10.1098/rstb.2015.0178.

[18] Copernicus Climate Change Service, Climate bulletin november, available at https://climate.copernicus.eu/copernicus-november-2023-remarkable-year-continues-warmest-boreal-autumn-2023-will-be-warmest-year (2023).

[19] M. T. Ballew, A. Leiserowitz, C. Roser-Renouf, S. A. Rosenthal, J. E. Kotcher, J. R. Marlon, E. Lyon, M. H. Goldberg, E. W. Maibach, Climate change in the American mind: Data, tools, and trends, Environment: Science and Policy for Sustainable Development 61 (3) (2019) 4–18. doi:10.1080/00139157.2019.1589300.

[20] European Commission, Special Eurobarometer 538: Climate change, last Accessed: April 7, 2025; available at https://climate.ec.europa.eu/system/files/2023-07/citizen_support_report_2023_en.pdf (2023).

[21] K. Mulvey, S. Shulman, D. Anderson, N. Cole, J. Piepenburg, J. Sideris, The climate deception dossiers: internal fossil fuel industry memos reveal decades of corporate disinformation, available at https://www.ucsusa.org/resources/climate-deception-dossiers (2015).

[22] R. J. Brulle, Institutionalizing delay: foundation funding and the creation of us climate change counter-movement organizations, Climatic Change 122 (2014) 681–694. doi:10.1007/s10584-013-1018-7.

[23] C. Boussalis, T. G. Coan, Text-mining the signals of climate change doubt, Global Environmental Change 36 (2016) 89–100. doi:10.1016/j.gloenvcha.2015.12.001.

[24] J. A. Layzer, Open for Business: Conservatives' Opposition to Environmental Regulation, The MIT Press, 2012.

[25] J. M. Turner, The Republican reversal: conservatives and the environment from Nixon to Trump, Harvard University Press, 2018.

[26] N. Oreskes, E. M. Conway, Merchants of doubt: How a handful of scientists obscured the truth on issues from tobacco smoke to global warming, Bloomsbury Publishing USA, 2011.

[27] J. L. Powell, The inquisition of climate science, Columbia University Press, 2011.

[28] A. Bessi, F. Petroni, M. D. Vicario, F. Zollo, A. Anagnostopoulos, A. Scala, G. Caldarelli, W. Quattrociocchi, Homophily and polarization in the age of misinformation, The European Physical Journal Special Topics 225 (2016) 2047–2059. doi:10.1140/epjst/e2015-50319-0.

[29] P. Barberá, Birds of the same feather tweet together: Bayesian ideal point estimation using Twitter data, Political Analysis 23 (1) (2015) 76–91. doi:10.1093/pan/mpu011.

[30] M. Conover, J. Ratkiewicz, M. Francisco, B. Gonçalves, F. Menczer, A. Flammini, Political polarization on Twitter, in: Proceedings of the International AAAI Conference on Web and Social Media, Vol. 5, 2011, pp. 89–96. doi:10.1609/icwsm.v5i1.14126.

[31] H. T. Williams, J. R. McMurray, T. Kurz, F. Hugo Lambert, Network analysis reveals open forums and echo chambers in social media discussions of climate change, Global Environmental Change 32 (2015) 126–138. doi:10.1016/j.gloenvcha.2015.03.006.

[32] E. Bakshy, S. Messing, L. A. Adamic, Exposure to ideologically diverse news and opinion on Facebook, Science 348 (6239) (2015) 1130–1132. doi:10.1126/science.aaa1160.

[33] L. Jasny, J. Waggle, D. R. Fisher, An empirical examination of echo chambers in us climate policy networks, Nature Climate Change 5 (8) (2015) 782–786. doi:10.1038/nclimate2666.

[34] M. Falkenberg, A. Galeazzi, M. Torricelli, N. Di Marco, F. Larosa, M. Sas, A. Mekacher, W. Pearce, F. Zollo, W. Quattrociocchi, A. Baronchelli,

Growing polarization around climate change on social media, Nature Climate Change 12 (12) (2022) 1114–1121. doi:10.1038/s41558-022-01527-x.

[35] R. E. Dunlap, A. M. McCright, J. H. Yarosh, The political divide on climate change: Partisan polarization widens in the US, Environment: Science and Policy for Sustainable Development 58 (5) (2016) 4–23. doi:10.1080/00139157.2016.1208995.

[36] Pew Research Center, What the data says about Americans' views of climate change, available at `https://www.pewresearch.org/short-reads/2023/08/09/what-the-data-says-about-americans-views-of-climate-change` (2023).

[37] J. M. Smith, Game theory and the evolution of behaviour, Proceedings of the Royal Society of London. Series B. Biological Sciences 205 (1161) (1979) 475–488. doi:10.1098/rspb.1979.0080.

[38] J. Hofbauer, K. Sigmund, et al., Evolutionary games and population dynamics, Cambridge University Press, 1998.

[39] A. McAvoy, Y. Mori, J. B. Plotkin, Selfish optimization and collective learning in populations, Physica D 439 (2022) 133426. doi:10.1016/j.physd.2022.133426.

[40] Y. Wu, G. Yang, Y. Li, Z. Zhang, J. Li, S. Zhang, Evolution of cooperation in multigames on interdependent networks, Physica D 447 (2023) 133692. doi:10.1016/j.physd.2023.133692.

[41] M. Ye, L. Zino, A. Rizzo, M. Cao, Game-theoretic modeling of collective decision making during epidemics, Physical Review E 104 (2021) 024314. doi:10.1103/PhysRevE.104.024314.

[42] K. Frieswijk, L. Zino, M. Ye, A. Rizzo, M. Cao, A mean-field analysis of a network behavioral–epidemic model, IEEE Control Systems Letters 6 (2022) 2533–2538. doi:10.1109/LCSYS.2022.3168260.

[43] S. N. Chowdhury, S. Kundu, M. Perc, D. Ghosh, Complex evolutionary dynamics due to punishment and free space in ecological multigames, Proceedings of the Royal Society A: Mathematical, Physical and Engineering Sciences 477 (2252) (2021) 20210397. doi:10.1098/rspa.2021.0397.

[44] L. Shu, F. Fu, Determinants of successful mitigation in coupled social-climate dynamics, Proceedings of the Royal Society A: Mathematical, Physical and Engineering Sciences 479 (2280) (2023). doi:10.1098/rspa.2023.0679.

[45] J. S. Weitz, C. Eksin, K. Paarporn, S. P. Brown, W. C. Ratcliff, An oscillating tragedy of the commons in replicator dynamics with game-environment feedback, Proceedings of the National Academy of Sciences 113 (47) (2016) E7518–E7525. doi:10.1073/pnas.1604096113.

[46] Y. Xie, S. Chang, M. Yan, Z. Zhang, X. Wang, Environmental influences on cooperation in social dilemmas on networks, Physica A 492 (2018) 2027–2033. doi:10.1016/j.physa.2017.11.118.

[47] S. Qin, G. Zhang, H. Tian, W. Hu, X. Zhang, Dynamics of asymmetric division of labor game with environmental feedback, Physica A 543 (2020) 123550. doi:10.1016/j.physa.2019.123550.

[48] L. Gong, W. Yao, J. Gao, M. Cao, Limit cycles analysis and control of evolutionary game dynamics with environmental feedback, Automatica 145 (2022) 110536. doi:10.1016/j.automatica.2022.110536.

[49] H. Cheng, X. Meng, Multistability and hopf bifurcation analysis for a three-strategy evolutionary game with environmental feedback and delay, Physica A 620 (2023) 128766. doi:10.1016/j.physa.2023.128766.

[50] A. R. Tilman, J. B. Plotkin, E. Akçay, Evolutionary games with environmental feedbacks, Nature Communications 11 (1) (2020) 1–11. doi:10.1038/s41467-020-14531-6.

[51] P. W. Schultz, Changing behavior with normative feedback interventions: A field experiment on curbside recycling, Basic and Applied Social Psychology 21 (1) (1999) 25–36. doi:10.1207/s15324834basp2101_3.

[52] N. J. Goldstein, R. B. Cialdini, V. Griskevicius, A room with a viewpoint: Using social norms to motivate environmental conservation in hotels, Journal of Consumer Research 35 (3) (2008) 472–482. doi:10.1086/586910.

[53] J. M. Nolan, P. W. Schultz, R. B. Cialdini, N. J. Goldstein, V. Griskevicius, Normative social influence is underdetected, Personality and Social Psychology Bulletin 34 (7) (2008) 913–923. doi:10.1177/0146167208316691.

[54] S. Göckeritz, P. W. Schultz, T. Rendón, R. B. Cialdini, N. J. Goldstein, V. Griskevicius, Descriptive normative beliefs and conservation behavior: The moderating roles of personal involvement and injunctive normative beliefs, European Journal of Social Psychology 40 (3) (2010) 514–523. doi:10.1002/ejsp.643.

[55] K. Frieswijk, L. Zino, M. Cao, A. S. Morse, Modeling the co-evolution of climate impact and population behavior: A mean-field analysis, in: Proceedings of the 2023 IFAC World Congress, Vol. 56, 2023, pp. 7381–7386. doi:10.1016/j.ifacol.2023.10.355.

[56] R. B. Cialdini, N. J. Goldstein, Social influence: compliance and conformity, Annual Review of Psychology 55 (1) (2004) 591–621. doi:10.1146/annurev.psych.55.090902.142015.

[57] D. A. Levin, Y. Peres, E. L. Wilmer, Markov chains and mixing times, American Mathematical Society, Providence RI, US, 2006.

[58] P. Van Mieghem, J. Omic, R. Kooij, Virus spread in networks, IEEE/ACM Transactions On Networking 17 (1) (2009) 1–14. doi:10.1109/TNET.2008.925623.

[59] T. Kurtz, Solutions of ordinary differential equations as limits of pure jump markov processes, Journal of Applied Probability 7 (1970) 49–58. doi:10.2307/3212147.

[60] T. G. Kurtz, Limit theorems for sequences of jump Markov processes approximating ordinary differential processes, Journal of Applied Probability 8 (2) (1971) 344–356. doi:10.2307/3211904.

[61] G. Teschl, Ordinary differential equations and dynamical systems, Vol. 140, American Mathematical Society, 2012.

[62] D. J. Hofmann, J. H. Butler, P. P. Tans, A new look at atmospheric carbon dioxide, Atmospheric Environment 43 (12) (2009) 2084–2086. doi:10.1016/j.atmosenv.2008.12.028.

[63] P. Friedlingstein, et al., Global carbon budget 2023, Earth System Science Data 15 (2023) 1–69. doi:10.5194/essd-15-5301-2023.

[64] A. Davariashtiyani, M. Taherkhani, S. Fattahpour, S. Vitousek, Exponential increases in high-temperature extremes in north america, Scientific Reports 13 (1) (Nov. 2023). doi:10.1038/s41598-023-41347-3.

[65] M. Bergquist, M. Thiel, M. H. Goldberg, S. van der Linden, Field interventions for climate change mitigation behaviors: A second-order meta-analysis, Proceedings of the National Academy of Sciences 120 (13) (2023) e2214851120. doi:10.1073/pnas.2214851120.

[66] W. Young, K. Hwang, S. McDonald, C. J. Oates, Sustainable consumption: green consumer behaviour when purchasing products, Sustainable Development 18 (1) (2010) 20–31. doi:10.1002/sd.394.

[67] T. Goertzel, Belief in conspiracy theories, Political Psychology 15 (4) (1994) 731–742. doi:10.2307/3791630.

[68] M. Biddlestone, F. Azevedo, S. van der Linden, Climate of conspiracy: A meta-analysis of the consequences of belief in conspiracy theories

about climate change, Current Opinion in Psychology 46 (2022) 101390. doi:10.1016/j.copsyc.2022.101390.

[69] D. Freeman, F. Waite, L. Rosebrock, A. Petit, C. Causier, A. East, L. Jenner, A.-L. Teale, L. Carr, S. Mulhall, E. Bold, S. Lambe, Coronavirus conspiracy beliefs, mistrust, and compliance with government guidelines in england, Psychological Medicine 52 (2) (2022) 251–263. doi:10.1017/S0033291720001890.

[70] W. H. Sandholm, Population games and evolutionary dynamics, MIT press, 2010.

[71] G. Como, F. Fagnani, L. Zino, Imitation dynamics in population games on community networks, IEEE Transactions on Control of Network Systems 8 (1) (2020) 65–76. doi:10.1109/TCNS.2020.3032873.

[72] K. H. Schlag, Why imitate, and if so, how?, Journal of Economic Theory 78 (1) (1998) 130–156. doi:10.1006/jeth.1997.2347.

[73] T. R. Zentall, Imitation in animals: Evidence, function, and mechanisms, Cybernetics and Systems 32 (1–2) (2001) 53–96. doi:10.1080/019697201300001812.

[74] L. Zino, A. Rizzo, M. Porfiri, The impact of deniers on epidemics: A temporal network model, IEEE Control Syst. Lett. 7 (2023) 685–690. doi:10.1109/LCSYS.2022.3219772.

[75] A. Traulsen, C. Hauert, H. De Silva, M. A. Nowak, K. Sigmund, Exploration dynamics in evolutionary games, Proceedings of the National Academy of Sciences 106 (3) (2009) 709–712. doi:10.1073/pnas.0808450106.

[76] C. M. Bender, S. A. Orszag, Advanced Mathematical Methods for Scientists and Engineers I, Springer New York, 1999. doi:10.1007/978-1-4757-3069-2.

[77] M. Wiedermann, J. F. Donges, J. Heitzig, W. Lucht, J. Kurths, Macroscopic description of complex adaptive networks coevolving

with dynamic node states, Physical Review E 91 (5) (May 2015). doi:10.1103/physreve.91.052801.

[78] J. J. Kolb, F. Müller-Hansen, J. Kurths, J. Heitzig, Macroscopic approximation methods for the analysis of adaptive networked agent-based models: Example of a two-sector investment model, Physical Review E 102 (4) (2020). doi:10.1103/physreve.102.042311.

[79] United Nations Development Programme, Peoples' climate vote, available at `https://www.undp.org/publications/peoples-climate-vote` (2021).

[80] S. Vallone, E. F. Lambin, Public policies and vested interests preserve the animal farming status quo at the expense of animal product analogs, One Earth 6 (9) (2023) 1213–1226. doi:10.1016/j.oneear.2023.07.013.

[81] Greenpeace, Ticket prices of planes versus trains: A Europe-wide analysis, available at `https://greenpeace.at/uploads/2023/07/report-ticket-prices-of-planes-vs-trains-in-europe.pdf` (2023).

[82] European Commission, Farm to fork strategy: For a fair, healthy and environmentally-friendly food system, available at `https://food.ec.europa.eu/system/files/2020-05/f2f_action-plan_2020_strategy-info_en.pdf` (2020).

[83] European Parlement, COP28: Members of the European Parliament want to end all subsidies for fossil fuel globally by 2025, available at `https://www.europarl.europa.eu/news/en/press-room/20231117IPR12108/cop28-meps-want-to-end-all-subsidies-for-fossil-fuel-globally-by-2025` (2023).

[84] F. Della Rossa, D. Salzano, A. Di Meglio, F. De Lellis, M. Coraggio, C. Calabrese, A. Guarino, R. Cardona-Rivera, P. De Lellis, D. Liuzza, F. Lo Iudice, G. Russo, M. di Bernardo, A network model of Italy shows that inter-

mittent regional strategies can alleviate the COVID-19 epidemic, Nature Communications 11 (1) (2020) 5106. doi:10.1038/s41467-020-18827-5.

[85] M. Bin, P. Y. K. Cheung, E. Crisostomi, P. Ferraro, H. Lhachemi, R. Murray-Smith, C. Myant, T. Parisini, R. Shorten, S. Stein, L. Stone, Post-lockdown abatement of covid-19 by fast periodic switching, PLOS Computational Biology 17 (1) (2021) e1008604. doi:10.1371/journal.pcbi.1008604.

[86] F. Parino, L. Zino, M. Porfiri, A. Rizzo, Modelling and predicting the effect of social distancing and travel restrictions on COVID-19 spreading, Journal of the Royal Society Interface 18 (175) (2021) 20200875. doi:10.1098/rsif.2020.0875.

[87] B. G. Pachpatte, Inequalities for differential and integral equations, Elsevier, 1997.

[88] F. Blanchini, Set invariance in control, Automatica 35 (11) (1999) 1747–1767. doi:10.1016/S0005-1098(99)00113-2.

[89] T. Günther, I. Baeza Rojo, Introduction to vector field topology, in: Topological Methods in Data Analysis and Visualization VI: Theory, Applications, and Software, Springer, 2021, pp. 289–326.

Appendix A. Proof of Proposition 5.1

First, we observe that since $(y(0), z(0), \varepsilon(0)) \in [0,1) \times (0,1) \times \mathbb{R}_{>0}$ (by Assumption 5.2), continuity ensures that there exists a $\hat{t} \in \mathbb{R}_{>0}$ such that $(y(t), z(t), \varepsilon(t)) \in [0,1) \times (0,1) \times \mathbb{R}_{>0}$, for all $t \in [0, \hat{t}]$. Here, we use the fact that Eq. (17) is locally Lipschitz-continuous around the initial condition and that, by Eq. (17a), $\dot{y}(0) \geq 0$ if $y(0) = 0$, which implies that $y(\hat{t}) \geq 0$. Eq. (17c) provides an intuitive bound on the maximal growth of $\varepsilon(t)$ up to time $\hat{t}$. In fact, since $y(t) \in [0,1]$ and $z(t) \in [0,1]$ for $t \in [0, \hat{t}]$, we bound $\dot{\varepsilon} \leq (\gamma - \tau)\varepsilon$, which implies by the Grönwall-Bellman inequality [87] that $\varepsilon(t) \leq \varepsilon(0) e^{(\gamma-\tau)t}$,

for all $t \in [0, \hat{t}]$. Next, we observe from Eq. (17a) that the third term of $\dot{y}(t)$ (the only negative term) vanishes as $y \to 0$. This implies that $\dot{y}$ is either positive or vanishing in a (right) neighbourhood of $y = 0$, implying by continuity that there exists a finite time-increment $\Delta t \in \mathbb{R}_{>0}$ such that $y(t)$ cannot become negative in the time-interval $[\hat{t}, \hat{t} + \Delta t]$. In a symmetric fashion, the first two terms of Eq. (17a) vanish as $y \to 1$, implying that $\dot{y}$ is either negative or vanishing in a (left) neighbourhood of $y = 1$. The same reasoning as used above implies that $y(t)$ cannot exceed 1 in the time interval $[\hat{t}, \hat{t} + \Delta t]$. Applying a similar argument to Eq. (17b), we obtain the same properties for $z(t)$ over the time interval $[\hat{t}, \hat{t} + \Delta t]$. Then, being $y(t) \in [0, 1]$ and $z(t) \in [0, 1]$ for all $t \in [\hat{t}, \hat{t} + \Delta t]$, it holds $\varepsilon \geq -\tau\varepsilon$, which implies (using again the Grönwall-Bellman inequality) that $\varepsilon(t)$ remains positive for all $t \in [\hat{t}, \hat{t} + \Delta t]$. Adopting recursively such an argument allows us to arbitrarily extend the time-interval for which $(y(t), z(t), \varepsilon(t)) \in [0, 1) \times (0, 1) \times \mathbb{R}_{>0}$, ultimately guaranteeing that i) $y(t) \in [0, 1)$, $z(t) \in (0, 1)$, and $\varepsilon(t) \in \mathbb{R}_{>0}$ for any finite time, and ii) $\varepsilon(t)$ cannot diverge in finite time.

Next, we prove by contradiction that $\varepsilon(t)$ cannot grow unbounded to $+\infty$. To this aim, we assume that $\varepsilon(t) \to \infty$ (which we know cannot happen in finite time) and we demonstrate that this assumption leads to a contradiction. From Eq. (17c), we bound

$$\dot{\varepsilon} \leq (\gamma(1 - (1 - d)z) - \tau)\varepsilon, \tag{A.1}$$

where we removed the term $-y\varepsilon$, which is clearly non-positive, yielding the above inequality. Let $\bar{z} = \frac{1}{1-d}(1 - \frac{\tau}{\gamma})$ and observe that necessarily $\bar{z} < 1$, as $d < \frac{\tau}{\gamma}$ (item iii of Assumption 5.1). For any $z > \bar{z}$, the bound in Eq. (A.1) implies that $\dot{\varepsilon} < 0$. Therefore, since $\varepsilon(t) \to \infty$, it must be satisfied that z cannot be definitively larger than $\bar{z}$. Formally, for any $\bar{t} \in \mathbb{R}_{\geq 0}$ there exists $t \geq \bar{t}$ such that $z(t) \leq \bar{z}$. Below, we will show how such a necessary condition would lead to a contradiction.

In fact, from Eq. (17b), we can bound $\dot{z} > -(1+\kappa)z$. Hence, by the Grönwall-Bellman inequality [87], $z(t) \geq z(0)e^{-(1+\kappa)t} > 0$ for all $t \in \mathbb{R}_{\geq 0}$. Next, from

Eq. (17b), we obtain another bound

$$\dot{z} \geq \big((1-d)\mu\varepsilon(1-z) - 1 - \kappa\big)z. \tag{A.2}$$

Since $\varepsilon(t) \to \infty$, the limit definition implies that there exists $\tilde{t} \in \mathbb{R}_{\geq 0}$ such that $\varepsilon(t) > \frac{2+\kappa}{\mu(\frac{\tau}{\gamma}-d)}$ for all $t \geq \tilde{t}$. Inserting this inequality into Eq. (A.2), we find that for all $t \geq \tilde{t}$,

$$\dot{z} > \Big((1-d)(1-z)\frac{2+\kappa}{\frac{\tau}{\gamma}-d} - 1 - \kappa\Big)z. \tag{A.3}$$

When $z(t) \leq \bar{z}$, we have $(1-d)(1-z) \geq \frac{\tau}{\gamma} - d$, and Eq. (A.3) yields $\dot{z} \geq z > 0$. When $z(t) \leq \bar{z}$, the Grönwall-Bellman inequality [87] yields $z(t) \geq z(\tilde{t})e^{t-\tilde{t}}$ for any $t \geq \tilde{t}$. Hence, for any $t \geq \tilde{t}$, either $z(t) > \bar{z}$ or $z(t) \geq z(\tilde{t})e^{t-\tilde{t}} \geq z(0)e^{-(2+\kappa)\tilde{t}+t} > 0$. Here, the latter implies that there exists $\hat{t} = \log(\bar{z}/z(0)) + (2+\kappa)\tilde{t}$ such that necessarily $z(t) > \bar{z}$ for $t > \hat{t}$. However, this is in contradiction with the observation that for any $\bar{t} \in \mathbb{R}_{\geq 0}$ there exists $t \geq \bar{t}$ with $z(t) < \bar{z}$, implying that $\varepsilon(t)$ cannot grow unbounded towards $+\infty$ and is bounded by some $\bar{\varepsilon} \in \mathbb{R}_{>0}$.

Thus, $\varepsilon(t)$ is bounded and Lipschitz-continuous (since it is the solution of an ODE). Note that $\dot{\varepsilon} = 0$ for $\varepsilon = 0$, so $\varepsilon(t) \in \mathbb{R}_{\geq 0}$ for all $t \in \mathbb{R}_{\geq 0}$. We observe that on the boundary $y = 0$, we have $\dot{y} = (1-d)(1-\theta)((1-d)z+\mu\varepsilon+\alpha)z \geq 0$, whereas $\dot{y} = -((1-d)(1-z)+\kappa)(1-d)(1-\theta)(1-z) \leq 0$ on the boundary $y = 1$. Similarly, we find $\dot{z} = d^2(1-\theta)y^2 \geq 0$ if $z = 0$, and $\dot{z} = -(d(1-y)+\kappa)d(1-\theta)(1-y) \leq 0$ on the boundary $z = 1$. Hence, the vector field is Lipschitz-continuous and points towards the interior of $[0,1]^2$. Thus, Nagumo's Theorem guarantees positive invariance of the compact domain $[0,1]^2$ for the pair of variables (y,z) [88]. □

Appendix B. Proof of Proposition 5.3

Let Assumption 5.1 hold, so $\tau < \gamma$, $\kappa > \alpha + 1$, and $d < \frac{\tau}{\gamma}$. Suppose that $(y(0), z(0), \varepsilon(0)) \in [0,1) \times (0,1) \times \mathbb{R}_{>0}$. By Proposition 5.1, $(y(0), z(0)) \in [0,1] \times [0,1]$ for all $t \in \mathbb{R}_{\geq 0}$ for any initial condition with $(y(0), z(0)) \in [0,1) \times (0,1)$. We will now show that it is impossible to reach the boundaries $y = 1$, $z = 0$, $z = 1$, and $\varepsilon = 0$ if $(y(0), z(0), \varepsilon(0)) \in [0,1) \times (0,1) \times \mathbb{R}_{>0}$. Note that

$2(dy+(1-d)z)-\kappa-1 \leq 1-\kappa < 0$. Hence, for $y \in (0,1)$ we have $\dot{y} < 0$, so y converges to 0 where $\dot{y} = 0$. This implies that if $y(0) \in [0,1)$, then $y(t) \in [0,1)$ for all $t \in \mathbb{R}_{\geq 0}$. Next, observe that for $z < 1$ and $\varepsilon \leq \frac{1}{\mu}(\kappa - \alpha - 1)$, we have $2(dy+(1-d)z)+\mu\varepsilon+\alpha-\kappa-1 < \mu\varepsilon+\alpha-\kappa+1 \leq 0$. Thus, for $z \in (0,1)$ and $\varepsilon \leq \frac{1}{\mu}(\kappa-\alpha-1)$, we have

$$\dot{z} = z(1-z)(2(dy+(1-d)z)+\mu\varepsilon+\alpha-\kappa-1) < 0. \tag{B.1}$$

Hence, for $z < 1$, z can only approach the border $z = 1$ for $\varepsilon > \frac{1}{\mu}(\kappa-\alpha-1)$. Suppose that there exists a trajectory $(y(t), z(t), \varepsilon(t))$ that enters the region

$$\mathcal{R} := [0,1] \times [1-\delta, 1] \times \left(\frac{1}{\mu}(\kappa-\alpha-1), \varepsilon(t_0)\right] \tag{B.2}$$

at a time t_0, where $\delta \in \big(0, 1 - \frac{1}{1-d}\big(1-\frac{\tau}{\gamma}\big)\big)$ is arbitrarily infinitesimally small. Here, note that $d < \frac{\tau}{\gamma}$ implies that $\frac{1}{1-d}\big(1-\frac{\tau}{\gamma}\big) < 1$. We will now show that $z(t)$ cannot reach the boundary $z = 1$. Observe that for $z \geq 1-\delta > \frac{1}{1-d}\big(1-\frac{\tau}{\gamma}\big)$, we have

$$\gamma(1-dy-(1-d)z)-\tau < \gamma(1-dy-(1-\tfrac{\tau}{\gamma}))-\tau = -\gamma dy \leq 0, \tag{B.3}$$

so $\dot{\varepsilon} < 0$ in $\mathcal{R}$ and the trajectory cannot exit $\mathcal{R}$ from above. Since $\varepsilon(t) \leq \varepsilon(t_0)$ in $\mathcal{R}$, we have

$$\dot{z} = z(1-z)(2(dy+(1-d)z)+\mu\varepsilon+\alpha-\kappa-1) \leq (1-z)(\mu\varepsilon(t_0)+\alpha-\kappa+1). \tag{B.4}$$

Thus, there exists a constant $p := \mu\varepsilon(t_0)+\alpha-\kappa+1 > 0$ such that $\dot{z} \leq p(1-x)$. Next, define $u(t) = 1 - z(t)$. Then, $\dot{z} \leq p(1-z)$ is equivalent to $-\dot{u} \leq -p(-u)$. Employing the Grönwall-Bellman inequality [87] gives $-u(t) \leq -u(t_0)e^{-p(t-t_0)}$, or equivalently, $z(t) \leq 1 - \delta e^{-p(t-t_0)} < 1$ for any $t \geq t_0$. Furthermore, observe that in $\mathcal{R}$,

$$\dot{\varepsilon} \leq -(\tau-\gamma(1-(1-d)(1-\delta)))\varepsilon < -\frac{1}{\mu}(\tau-\gamma(1-(1-d)(1-\delta)))(\kappa-\alpha-1), \tag{B.5}$$

where $\tau - \gamma(1-(1-d)(1-\delta)) > 0$ since $\delta < 1 - \frac{1}{1-d}\big(1-\frac{\tau}{\gamma}\big)$. Hence,

$$|\dot{\varepsilon}| > \frac{1}{\mu}\big(\tau-\gamma(1-(1-d)(1-\delta))\big)\big(\kappa-\alpha-1\big). \tag{B.6}$$

As the length of the ε-axis in $\mathcal{R}$ is less than $\varepsilon(t_0) - \frac{1}{\mu}(\kappa - \alpha - 1)$, there exists

$$t^* < \frac{\mu\varepsilon(t_0) - (\kappa - \alpha - 1)}{(\tau - \gamma(1 - (1-d)(1-\delta)))(\kappa - \alpha - 1)} \tag{B.7}$$

such that $\varepsilon(t_0 + t^*) \leq \frac{1}{\mu}(\kappa - \alpha - 1)$. At time $t_0 + t^*$, we have $z(t_0 + t^*) \leq 1 - \delta e^{-pt^*} < 1$, and the trajectory reaches the region $\mathcal{S} := [0,1] \times [1-\delta, 1] \times \left[0, \frac{1}{\mu}[\kappa - \alpha - 1]\right]$. Since $\dot{z} < 0$ for $\varepsilon \leq \frac{1}{\mu}(\kappa - \alpha - 1)$, the trajectory will be repelled from the boundary $z = 1$. Thus, if $z(0) \in (0,1)$, then $z(t) < 1$ for all $t \in \mathbb{R}_{\geq 0}$. Likewise, we can show that it is impossible to reach the boundary $z = 0$ if $z(0) > 0$ and $\varepsilon(0) > 0$.

We will now show that if $\varepsilon(0) \in \mathbb{R}_{>0}$, then $\varepsilon(t) \in \mathbb{R}_{>0}$ for all $t \in \mathbb{R}_{\geq 0}$. Observe that $\dot{\varepsilon} < 0$ if and only if $\varepsilon > 0$ and $dy + (1-d)z > 1 - \frac{\tau}{\gamma}$. Let us assume that there exists a trajectory that reaches $\varepsilon = \tilde{\delta}$ at a time $\hat{t}$, where $\tilde{\delta} \in \left(0, \frac{1}{\mu}(\kappa - \alpha - 1)\right)$ is arbitrarily infinitesimally small. We also assume that at time $\hat{t}$, y and z are such that $dy(\hat{t}) + (1-d)z(\hat{t}) > 1 - \frac{\tau}{\gamma}$, so $\dot{\varepsilon} < 0$. Next, note that for $z < 1$, $\dot{\varepsilon} = (\gamma(1 - dy - (1-d)z) - \tau)\varepsilon > -\tau\varepsilon$. Let us define $v(t) = -\varepsilon(t)$. The inequality $\dot{\varepsilon} > -\tau\varepsilon$ is equivalent to $\dot{v} < -\tau v$. Applying the Grönwall-Bellman inequality [87]) gives $v(t) < v(\hat{t})e^{-\tau(t-\hat{t})}$, or equivalently $\varepsilon(t) > \tilde{\delta}e^{-\tau(t-\hat{t})} > 0$ for $t \geq \hat{t}$. Hence, $\varepsilon = 0$ cannot be reached if $\varepsilon(0) \in \mathbb{R}_{>0}$. Furthermore, note that $\dot{z} < 0$ in the region for which $dy + (1-d)z > 1 - \frac{\tau}{\gamma}$ and $\varepsilon \leq \frac{1}{\mu}(\kappa - \alpha - 1)$. Combined with the fact that $\dot{y} < 0$ for $y \in (0,1)$, this means that there exists a time $\hat{t} + \tilde{t}$ with $\varepsilon(\hat{t} + \tilde{t}) > \tilde{\delta}e^{-\tau\tilde{t}} > 0$ such that $dy(\hat{t} + \tilde{t}) + (1-d)z(\hat{t} + \tilde{t}) \leq 1 - \frac{\tau}{\gamma}$, for which $\dot{\varepsilon} \geq 0$ and the trajectory will stop approaching the boundary $\varepsilon = 0$.

Thus, we have shown that if $(y(0), z(0), \varepsilon(0)) \in [0,1) \times (0,1) \times \mathbb{R}_{>0}$, then necessarily $(y(t), z(t), \varepsilon(t)) \in [0,1) \times (0,1) \times \mathbb{R}_{>0}$ for all $t \in \mathbb{R}_{\geq 0}$. □

Appendix C. Proof of Proposition 5.4

Let Assumption 5.1 hold, so $\tau < \gamma$, $\kappa > \alpha + 1$, and $d < \frac{\tau}{\gamma}$. Furthermore, let Assumption 5.2 hold, so $(y(0), z(0), \varepsilon(0)) \in [0,1) \times (0,1) \times \mathbb{R}_{>0}$. By Proposition 5.3, we then have $(y(t), z(t), \varepsilon(t)) \in [0,1) \times (0,1) \times \mathbb{R}_{>0}$ for all $t \in \mathbb{R}_{\geq 0}$. Solving $\dot{y} = 0$ gives $y = 0$ or $y = \frac{\kappa + 1 - 2(1-d)z}{2d}$. However, it follows from $z \leq 1$

and $\kappa > \alpha + 1$ that

$$y = \frac{\kappa + 1 - 2(1-d)z}{2d} \geq \frac{\kappa + 1 - 2(1-d)}{2d} = 1 + \frac{\kappa - 1}{2d} > 1 + \frac{\alpha}{2d} > 1. \quad \text{(C.1)}$$

Hence, $y = 0$ is the only solution to $\dot{y} = 0$. Consider $y = 0$. Solving $\dot{z} = 0$ yields $z = \frac{\kappa+1-\alpha-\mu\varepsilon}{2(1-d)}$. For $z = \frac{\kappa+1-\alpha-\mu\varepsilon}{2(1-d)}$, $\dot{\varepsilon} = 0$ if $\varepsilon = \frac{1}{\mu}\big(\frac{2\tau}{\gamma} + \kappa - \alpha - 1\big)$. Plugging $\varepsilon = \frac{1}{\mu}\big(\frac{2\tau}{\gamma} + \kappa - \alpha - 1\big)$ into $z = \frac{\kappa+1-\alpha-\mu\varepsilon}{2(1-d)}$ gives the equilibrium in Eq. (23). Observe that $z = \frac{1}{1-d}\big(1 - \frac{\tau}{\gamma}\big) < 1$ iff $d < \frac{\tau}{\gamma}$, so this equilibrium exists by Assumption 5.1. Next, we study the local stability characteristics of the unique equilibrium in Eq. (23). We define the change of variables

$$\bar{z} := z - \tfrac{1}{1-d}\left(1 - \tfrac{\tau}{\gamma}\right), \quad \text{and} \quad \bar{\varepsilon} := \varepsilon - \tfrac{1}{\mu}\left(\tfrac{2\tau}{\gamma} + \kappa - \alpha - 1\right). \quad \text{(C.2)}$$

Linearising the system in Eq. (22) around this equilibrium is equivalent to linearising the system $(y, \bar{z}, \bar{\varepsilon})$ around the origin, which gives a Jacobian matrix with eigenvalues $-\big(\kappa + \frac{2\tau}{\gamma} - 1\big) < 0$, and

$$\lambda_{1,2} = \phi \pm \sqrt{\phi^2 - \phi\left(2\tau + \gamma(\kappa - \alpha - 1)\right)}, \quad \text{(C.3)}$$

with $\phi := (1 - \frac{\tau}{\gamma})(1 - \frac{1}{1-d}(1 - \frac{\tau}{\gamma}))$. Note that Assumption 5.1 implies that $1 - \frac{\tau}{\gamma} > 0$ and $1 - \frac{1}{1-d}\big(1 - \frac{\tau}{\gamma}\big) > 0$. Hence, if the radicand in Eq. (C.3) is negative, we have $\lambda_{1,2} \in \mathbb{C}$ with $\mathrm{Re}(\lambda_1) = \mathrm{Re}(\lambda_2) = \phi > 0$, implying that the equilibrium in Eq. (23) is a repelling spiral saddle point [89]. If the radicand in Eq. (C.3) is non-negative, we have $\sqrt{\phi^2 - \phi(2\tau + \gamma(\kappa - \alpha - 1))} < \phi$, as $\kappa > \alpha + 1$. Thus, if the radicand is non-negative, it follows that $\lambda_{1,2} \in \mathbb{R}_{>0}$, implying that the equilibrium in Eq. (23) is a repelling saddle point [89]. A repelling saddle point has one inflow direction and a two-dimensional plane with outflow behaviour. As $\dot{y} < 0$ for $y \in (0, 1)$, the direction of inflow is along the y-axis. □